

Discovering Sex and Age Implicator Edges in the Human Connectome

László Keresztes^{a,**}, Evelin Szögi^{a,**}, Bálint Varga^a, Vince Grolmusz^{a,b,*}

^aPIT Bioinformatics Group, Eötvös University, H-1117 Budapest, Hungary

^bUratim Ltd., H-1118 Budapest, Hungary

Abstract

Determining important vertices in large graphs (e.g., Google’s PageRank in the case of the graph of the World Wide Web) facilitated the construction of excellent web search engines, returning the most important hits corresponding to the submitted user queries. Interestingly, finding important edges – instead of vertices – in large graphs has received much less attention until now. Here we examine the human structural braingraph (or connectome), identified by diffusion magnetic resonance imaging (dMRI) methods, with edges connecting cortical and subcortical gray matter areas and weighted by fiber strengths, measured by the number of the discovered fiber tracts along the edge. We identify several “single” important edges in these braingraphs, whose high or low weights imply the sex or the age of the subject observed. We call these edges implicator edges since solely from their weight, one can infer the sex of the subject with more than 67 % accuracy or their age group with more than 62% accuracy. We argue that these brain connections are the most important ones characterizing the sex or the age of the subjects. Surprisingly, the edges implying the male sex are mostly located in the anterior parts of the brain, while those implying the female sex are mostly in the posterior regions. Additionally, most of the inter-hemispheric implicator edges are male ones, while the intra-hemispheric ones are predominantly female edges. Our pioneering method for finding the sex- or age implicator edges can also be applied for characterizing other biological and medical properties, including neurodegenerative- and psychiatric diseases besides the sex or the age of the subject, if large and high-quality neuroimaging datasets become available. We emphasize that our contribution identifies statistically valid single brain connections related to the sex and the age of the subjects in a large and robust dataset. To our knowledge, our results are unprecedented in this aspect.

Introduction

Introducing novel tools in the life sciences has the ultimate goal of finding new pharmaceuticals and therapies for human diseases. In spite of the astronomical increase of the funding of medical research, the yearly number of the globally approved new drugs from the eighties through the first decade of the new century was decreasing on average ([1], Figure 1). This observation shows that mankind needs to exploit more aggressively the possibilities, which groundbreaking technologies, methods, and knowledge offered to life sciences.

One particular challenge is discovering the relations between the fine structure and the function of our brain. For this goal, among other important tools, magnetic resonance imaging (MRI) has a special role: the number of available MRI scanners is constantly increasing worldwide in hospitals and research facilities, and the accompanying data acquisition procedure is non-invasive and harmless.

*Corresponding author

**Joint first authors

Email addresses: keresztes@pitgroup.org (László Keresztes), szogi@pitgroup.org (Evelin Szögi), balorkany@pitgroup.org (Bálint Varga), grolmusz@pitgroup.org (Vince Grolmusz)

Therefore, the cerebral MRI has the potential application in numerous conditions, assuming we know what to look for in the data.

A multitude of recent publications examine the human structural connectome, i.e., the macroscopic-scale cerebral connections between the distinct brain areas [2, 3, 4]. These connections were mapped by applying diffusion MRI (dMRI), and using an algorithmic workflow for mapping the braingraph [5, 6, 7, 8, 9].

Unfortunately, most contributions in this area present findings in the human structural connectome, which cannot be translated to the needs of the medical practice. Some contributions even use weakly defined philosophical terms in the analysis of these graphs instead of strict and clear notations. Our research group has pioneered in applying less philosophical and much more engineering-oriented, exact graph-theoretical terms and definitions, rooted in the classical (mathematical) graph theory, and applied widely in computer engineering [10]. For example, we have studied quantitative connectivity-related graph parameters, like the size of the balanced minimum cut, the measure of the graph expanding property, or the size of the minimum vertex cover in [11, 12, 13, 14], and proved that these parameters are significantly better in women's braingraphs than in men's [15, 11] (where the "better" adjective refers to the network connection properties, characterizing better interconnection networks, as defined and studied in [10, 16]; it is still not proven that better network parameters directly correspond to better brain functions). We have mapped the frequencies of the edges in consensus braingraphs in several settings [17, 18, 19], and discovered frequent subgraphs [20], frequent complete graphs [21] and frequent neighbor sets of one of the most widely studied brain areas, the hippocampus [22, 23].

In the medical practice, simpler markers would be much more applicable: for example, the strengths (defined in fiber numbers) of certain, *single* connections between specific brain areas can be measured relatively easily from the diffusion MRIs, and these single edge strengths may imply relevant biological or medical conditions. Similarly, evaluating the consequences of cerebral traumas is easier if we have strong statistical knowledge on the importance of distinct connections between the areas of the gray matter, which are affected by the traumas: that is, not only the importance of the cortical and subcortical gray matter areas need to be evaluated in trauma, but also the importance of the broken connections between these (potentially healthy) gray matter areas.

In the contribution [24] we have found very few edges with dramatic biological effects: we have shown that just 102 edges simply, by a linear relation, determine the sex of the subject, without errors, and, even more surprisingly, we described two superfeminine edges in the human connectome, whose high edge-weights imply the female sex of the subject, independently of the other edges. Similarly, in [24], we have identified two super-masculine edges with similar properties.

In the present work, we describe several *single* human brain connections, whose strengths have strong correlations with the sex or the age of the subjects. For example, the edge connecting the left superior parietal area with the Left-Caudate nucleus has very significantly ($p=10^{-30}$) more axonal tracts in females than in males, and by the observation of only that single edge, one can infer the sex of the subject with 67% accuracy; more exactly, the following implications are valid with 67% accuracy:

$$fn(\text{ left superiorparietal area, Left-Caudate }) \geq 1561 \implies \text{the subject is female};$$

and

$$fn(\text{ left superiorparietal area, Left-Caudate }) < 1561 \implies \text{the subject is male}.$$

Here fn denotes the number of observed axonal fibers (i.e., **fiber number**) in the edge.

Conversely, the edge connecting the left rostral middle frontal area with the left Caudate nucleus is very significantly stronger in males than in females; one can make sex-identification solely by observing that edge with 67% accuracy:

$fn(\text{left rostralmiddlefrontal area, Left-Caudate}) \geq 1464 \implies \text{the subject is male};$

and

$fn(\text{left rostralmiddlefrontal area, Left-Caudate}) < 1464 \implies \text{the subject is female}.$

For further implications, we refer to Tables 1 and 2 and the supporting Tables S1, S2, S3, S4, and S5 in the supporting material).

We argue that instead of the sex or the age of the subjects, other medical and biological attributes can also be described this way if the size and the quality of the underlying dataset allow that analysis. Here we were able to find these implications since we have used the high quality 1200 subjects data release of the Human Connectome Project [25], and computed the braingraphs with an unprecedentedly robust, error-correcting way [26]. Our robust source graphs are publicly available at <https://braingraph.org> [26].

Methods

The diffusion MRI data were recorded and made public by the Human Connectome Project's (HCP) website at <http://www.humanconnectome.org> [27] as the 1200-subjects public release. Our group constructed the braingraphs from the HCP data, which are analyzed in the present contribution. The details of the robust graph construction are described in [26]; here, we just concisely review the graph computation process of [26] as follows:

- (i) Parcellation was done by using the Connectome Mapper Tool Kit (CMTK) [5] with Lausanne2008 scheme, with labels https://github.com/LTS5/cmp_nipype/blob/master/cmtklib/data/parcellation/lausanne2008/ParcellationLausanne2008.xls. Five resolutions were computed, with 83, 129, 234, 463 and 1015 nodes.
- (ii) Probabilistic tractography with random seeding was performed by the MRtrix 0.3 tractography algorithm [28], with 10 repetitions for each subject. A graph edge $\{a, b\}$ connects vertex a , corresponding to a gray matter area A and b , corresponding to gray matter area B if in each of the 10 runs at least one axonal fiber was found by the tractography algorithm between areas A and B . In this case, because of the repeated runs, edge $\{a, b\}$ has 10 fiber numbers, several of them distinct, several of them equal.
- (iii) As a further error-correcting measure, for each edge, we considered the fiber numbers identified in the ten runs. Next, the minimum and the maximum values of the 10 fiber number values were thrown out as extremes, and the remaining 8 fiber numbers were averaged, and this average was assigned to the edge as its robust, averaged fiber number.

We were able to perform the computational steps above for 1064 subjects, each with 5 resolutions, with 83, 129, 234, 463, and 1015 nodes, respectively. The resulting braingraphs can be accessed at the <https://braingraph.org/cms/download-pit-group-connectomes/> site.

In the present work, we consider the coarsest, 83-node resolution of these 1064 robust braingraphs exclusively. The edges at the <https://braingraph.org/cms/download-pit-group-connectomes/> site carry three weights: (i) the number of fibers, denoted by fn ; (ii) the mean value of the fiber lengths (in mm) of the edge-defining fibers, denoted by fl ; the (iii) mean fractional anisotropy fa of the fibers [29].

Since the fiber number for each edge is an average of the eight of the ten tractography runs, even the fiber number fn is – typically – not an integer. From these weights, here we also introduce an electrical conductivity-related edge weight:

$$con = \frac{fn \cdot fa}{fl^2}.$$

The quantity above is slightly related to electrical conductivity, since it is proportional to the (fiber number) \times (fractional anisotropy) product, where fiber number fn can be seen as the “width” of the connection, and the fractional anisotropy as the “quality” of the connection, and it is inversely proportional to the square of the length of the connection.

The union of the edge-sets of 1064 graphs on 83 nodes has 1950 edges: that is, from the $\binom{83}{2} = 3403$ vertex-pairs, 1950 form edges in at least one of the 1064 graphs, the remaining vertex-pairs do not form edges (i.e., connections) in the graphs.

Implicator edges

In what follows, we will find single edges in the braingraph, whose weights imply the sex or the age of the subject, with accuracy greater than 60%. To our knowledge, no such single implicator edges in the human connectome were identified before the present work. For finding those edges, we will consider the 1950 weighted edges, which appear in at least one subject from 1064, and compare the distribution of their weights between the sexes or the age groups.

We intend to identify for each edge j and for each weighting method a cut-value, denoted by c below, such that the weight of the edge would discriminate between sexes or age groups if they are below or above the cut-value c . The list of the edges for which such cut-values exist with strong statistical significance is given in the tables and figures below.

Edge assessment

For the identification of the sex implicator edges, we consider the two-sample Kolmogorov-Smirnov test [30] with different edge weights. First, we describe the method in detail with abstract edge weights; then, we deal with the specific edge weights.

Let X be the matrix describing the edge weights for each subject: the 1064 rows of X correspond to the subjects, the 1950 columns to the edges. For each edge $j = 1, \dots, 1950$ we determined the empirical distribution functions for males and females, $F_{male,j}$ and $F_{female,j}$ as follows:

$$\begin{aligned} F_{male,j}(t) &= \frac{1}{n_m} \sum_{i \text{ male}} \mathbb{I}(X[i, j] < t) \\ F_{female,j}(t) &= \frac{1}{n_f} \sum_{i \text{ female}} \mathbb{I}(X[i, j] < t) \end{aligned}$$

Here, $n_m = 489$ is the number of males, and $n_f = 575$ is the number of females; \mathbb{I} is the indicator function, its value is 1 if the condition in its argument is satisfied, and 0 otherwise.

For each edge we computed the D_j value (the greatest absolute difference) of the two empirical distribution functions:

$$D_j = \sup_t |F_{male,j}(t) - F_{female,j}(t)|$$

For each edge j , our statistical null hypothesis was that $F_{male,j}$ and $F_{female,j}$ do not differ, and we rejected the null hypothesis if D_j is high enough (to be specified later). The corresponding p_j p-values were computed by the Python Scipy’s stats module [31].

The D_j statistics are related to the best separation of males and females based on the values of edge j . Let n_f be the number of females, n_m be the number of males, and let ACC be the accuracy of best separation. We can assume that in the best separation, females have higher values (the other direction is similar). Let c be the cut-value for the best separation, then:

$$ACC = \frac{n_m F_{male,j}(c) + n_f (1 - F_{female,j}(c))}{n_m + n_f}$$

If $n_m = n_f$, then:

$$ACC = \frac{1 + F_{male,j}(c) - F_{female,j}(c)}{2} = \frac{1 + D_j}{2}$$

Similarly if $n_m \approx n_f$, then:

$$ACC \approx \frac{1 + D_j}{2}$$

In the ideal case, when $n_m = n_f$, the edge with the lowest p-value is the best separator. When $n_m \approx n_f$, then edges with lower p-values are presumably better separators. Using the Kolmogorov-Smirnov test with the previous connection to ACC , we are searching for better separator edges with higher D_j statistics (and lower p_j values).

The best separation has a direction, and it enables us to define whether an edge is “male impicator” or “female impicator”:

- (i) An edge j is a female impicator edge with a fixed weight scheme if in the best separation females have higher weight values than the cut-value c , or male impicator edge if in the best separation males have higher weight values than the cut-value c . We will use this terminology for the impicator edges.

We call an edge significant if we reject the null hypothesis. It is possible that we call an edge significant falsely (type I error), that probability is controlled by the p-value. As we call more and more edges significant (because of low p-values), there is an increasing probability that at least one was falsely labeled as significant; this is the FWER (family-wise error rate). When we had the p_j value for each edge, we can rank them as the edge with the lowest p-value is the most significant. We applied the Holm-Bonferroni correction to control FWER [32].

In general, let H_{0j}, H_{1j} ($j = 1, \dots, m$) be m pairs of hypotheses, where H_{0j} is the null hypothesis for edge j (edge j is not significant or there is no difference in distributions) and H_{1j} is the alternative hypothesis for edge j (edge j is significant or there is a difference in distributions). Let m_0 be the number of true null hypotheses (number of j s, where H_{0j} is true). We can assume, that these are the first m_0 hypotheses. Let A_j be the event, that we make a type I error on edge j (we call edge j significant, but H_{0j} is true). The p-values tell that $Pr(A_j) = p_j$. Writing the definition of FWER and using Boole’s inequality:

$$FWER = Pr\left(\bigcup_{j=1}^m A_j\right) = Pr\left(\bigcup_{j=1}^{m_0} A_j\right) \leq \sum_{j=1}^{m_0} Pr(A_j) = \sum_{j=1}^{m_0} p_j$$

If we define α and we set $\frac{\alpha}{m}$ on threshold for p-values (reject the null hypothesis if $p_j \leq \frac{\alpha}{m}$), then we control FWER with α :

$$FWER \leq \sum_{j=1}^{m_0} p_j \leq m_0 \frac{\alpha}{m} \leq \alpha$$

This Holm-Bonferroni correction works in all cases of dependencies in the tests. This correction is sometimes too strict; there is no edge that $p_j \leq \frac{\alpha}{m}$ with a regular value for α (e.g. $\alpha \leq 0.05$).

In our study, with $\alpha < 1.95 \times 10^{-5}$, 158 significant edges were found with the fn edge weight, so the probability that any of these 158 (fn weighted) edges do not differ between males and females is less than 1.95×10^{-5} . With $\alpha = 10^{-8} \times m$, where $m = 1950$ the number of tests, thus each significant edges must have a p-value lower than 10^{-8} .

See Table 1 for the most significant 30 impicator edges based on fn weight and the supporting Table S1 for the 158 significant edges with the fn weight.

For the visualization of the locations of the significant edges in the human brain, we refer to Figures 1 and 2 and supporting Figures S1, S2, S3, and S4 in the supporting material. In the figures, male impicator edges are colored to blue, while female impicator edges to red.

Discussion and Results

Significant edges weighted by fiber number

In Table 1 we present the 30 most significant edges (from the 158 ones in Table S1). The index column refers to the ranking, *Vertex 1* and *Vertex 2* are the corresponding brain areas connected by the edge, $M>F$ indicates a male impicator edge, that is, an edge, where the “male” implication is valid if the weight of the edge is larger than the c *cut-value*, while $M<F$ indicates a female impicator edge, that is, an edge where the “female” implication is valid if the weight of the edge is larger than the c *cut-value*. The p_{-ks} and D_{-ks} mean the Kolmogorov-Smirnov p-value and statistics for an edge. ACC denotes the accuracy of the best separation, ACC_{-ks} denotes the $\frac{1}{2}(1 + D_{-ks})$ Kolmogorov-Smirnov estimation for best separation. $FWER$ in the k th row shows the FWER upper bound for the first k edges.

The best possible classification available using only one edge is 67% accurate, and better than 65% accuracy available for more than 15 edges: these edges have the highest discriminative power.

Vertex 1	Vertex 2	Male ? Female	c	p_{-ks}	D_{-ks}	ACC	ACC_{-ks}	$FWER$
1 lh.superiorparietal	Left-Caudate	M<F	1561	1e-30	0.36	0.67	0.68	2e-27
2 lh.rostralmiddlefrontal	Left-Caudate	M>F	1464	8e-29	0.35	0.67	0.67	1e-25
3 rh.caudanteriorcingulate	lh.rostralmiddlefrontal	M>F	3	4e-28	0.34	0.67	0.67	8e-25
4 lh.precuneus	Left-Caudate	M<F	436	4e-27	0.34	0.67	0.67	9e-24
5 lh.parsopercularis	lh.inferiorparietal	M<F	2	8e-27	0.33	0.67	0.67	2e-23
6 rh.rostralmiddlefrontal	Right-Caudate	M>F	1544	5e-25	0.32	0.67	0.66	9e-22
7 rh.precuneus	Right-Caudate	M<F	335	1e-24	0.32	0.66	0.66	2e-21
8 rh.rostralanteriorcingulate	rh.caudanteriorcingulate	M>F	18	2e-24	0.32	0.66	0.66	3e-21
9 rh.caudanteriorcingulate	Right-Caudate	M>F	2462	3e-24	0.32	0.66	0.66	6e-21
10 lh.rostralanteriorcingulate	lh.caudanteriorcingulate	M>F	58	4e-24	0.32	0.66	0.66	8e-21
11 rh.parsopercularis	rh.inferiorparietal	M<F	20	5e-24	0.32	0.65	0.66	1e-20
12 Right-Putamen	Right-Amygdala	M>F	49	6e-22	0.30	0.65	0.65	1e-18
13 rh.superiortemporal	rh.transversetemporal	M>F	74	1e-21	0.30	0.65	0.65	3e-18
14 Right-Caudate	lh.rostralmiddlefrontal	M>F	5	7e-21	0.30	0.64	0.65	1e-17
15 rh.precuneus	Right-Hippocampus	M<F	1462	2e-20	0.29	0.64	0.65	4e-17
16 rh.precuneus	Right-Putamen	M<F	290	2e-20	0.29	0.65	0.65	4e-17
17 rh.superiorparietal	Right-Caudate	M<F	830	2e-20	0.29	0.65	0.65	4e-17
18 lh.posteriorcingulate	Left-Putamen	M<F	658	3e-20	0.29	0.64	0.65	5e-17
19 lh.parsopercularis	lh.supramarginal	M<F	145	5e-20	0.29	0.64	0.64	9e-17
20 Left-Putamen	Left-Amygdala	M>F	39	6e-20	0.29	0.65	0.64	1e-16
21 rh.insula	Right-Amygdala	M>F	19	6e-19	0.28	0.64	0.64	1e-15
22 lh.fusiform	Left-Hippocampus	M<F	310	7e-19	0.28	0.64	0.64	1e-15
23 lh.inferiorparietal	Left-Thalamus-Proper	M<F	1249	2e-18	0.28	0.64	0.64	3e-15
24 lh.lingual	Left-Putamen	M<F	9	6e-18	0.27	0.63	0.64	1e-14
25 rh.rostralanteriorcingulate	Right-Caudate	M>F	103	8e-18	0.27	0.64	0.64	1e-14
26 Right-Accumbens-area	Left-Thalamus-Proper	M>F	2	4e-17	0.27	0.64	0.63	7e-14
27 lh.inferiorparietal	Left-Putamen	M<F	246	1e-16	0.26	0.63	0.63	3e-13
28 rh.parsopercularis	lh.supramarginal	M<F	205	2e-16	0.26	0.63	0.63	4e-13
29 lh.parstriangularis	lh.rostralmiddlefrontal	M>F	266	2e-16	0.26	0.63	0.63	4e-13
30 lh.bankssts	Left-Hippocampus	M<F	325	2e-16	0.26	0.64	0.63	5e-13

Table 1: The 30 most significant sex impicator edges. The index column refers to the ranking, *Vertex 1* and *Vertex 2* are the corresponding brain areas connected by the edge, $M>F$ indicates an edge, where the “male” implication is valid if the weight of the edge is larger than the “ c ” *cut-value*, while $M<F$ indicates an edge where the “female” implication is valid if the weight of the edge is larger than the “ c ” *cut-value*. The p_{-ks} and D_{-ks} mean the Kolmogorov-Smirnov p-value and statistics for the edge. ACC denotes the accuracy of the “male” or “female” implication, ACC_{-ks} denotes the $\frac{1}{2}(1 + D_{-ks})$ Kolmogorov-Smirnov estimation for best separation accuracy. $FWER$ in the k th row shows the FWER upper bound for the first k edges.

We review some of the most significant sex impicator edges from Table 1 here. The higher fiber numbers of the edges between the caudate and the superior parietal regions imply the female sex in both hemispheres (Table 1, lines 1 and 17), with 67% and 65% accuracy, respectively.

In contrast, the higher fiber numbers in the edges between the caudate and rostral middle frontal regions in both hemispheres (Table 1, lines 2 and 6) imply the male sex with 67% accuracy.

In the literature, the endpoints of the edges in Table 1 frequently appeared in volumetric studies in conjunction with sex dimorphisms and sexual functions. It is not surprising that the caudate nucleus and the putamen appear several times in Table 1 as endpoints of impicator edges: the basal ganglia have a large number of sex steroid receptors, and they were demonstrated having sex dimorphisms in previous volumetric studies [33, 34]. Other volumetric studies have shown the sex difference in the development in the hippocampus vs. the amygdala: the amygdala volumes increase more in men and the hippocampus volumes more in women, during puberty [35]. Volumetric sex differences were also reported in the inferior parietal lobule in [36].

We emphasize that in our contribution, we identify statistically valid *brain connections* (and not just the volumes of the brain areas which were previously done by many sources) related to sex and age in a large, robust and coherent dataset.

Plots of the significant edges weighted by fiber numbers (fn)

In this section, we show the resulting plots of the significant edge selection method.

The blue edges are always the male impicator edges, and the red edges are the female impicator ones. This categorization is based on the best separation on the corresponding edge as we described.

Here we consider the most natural *fn* (fiber-number) weight. Figures with other weight functions can be found in the supporting material. We selected $\alpha = 1.95 \times 10^{-5}$ as the upper bound on FWER, which is the same as calling an edge significant if the p-value is lower than 10^{-8} . With this setting on α , 158 significant edges were found (see Table S1). Figure 1 shows their location.

It is striking that the male impicator edges are located mostly in the anterior, while the female edges in the posterior areas of the brain.

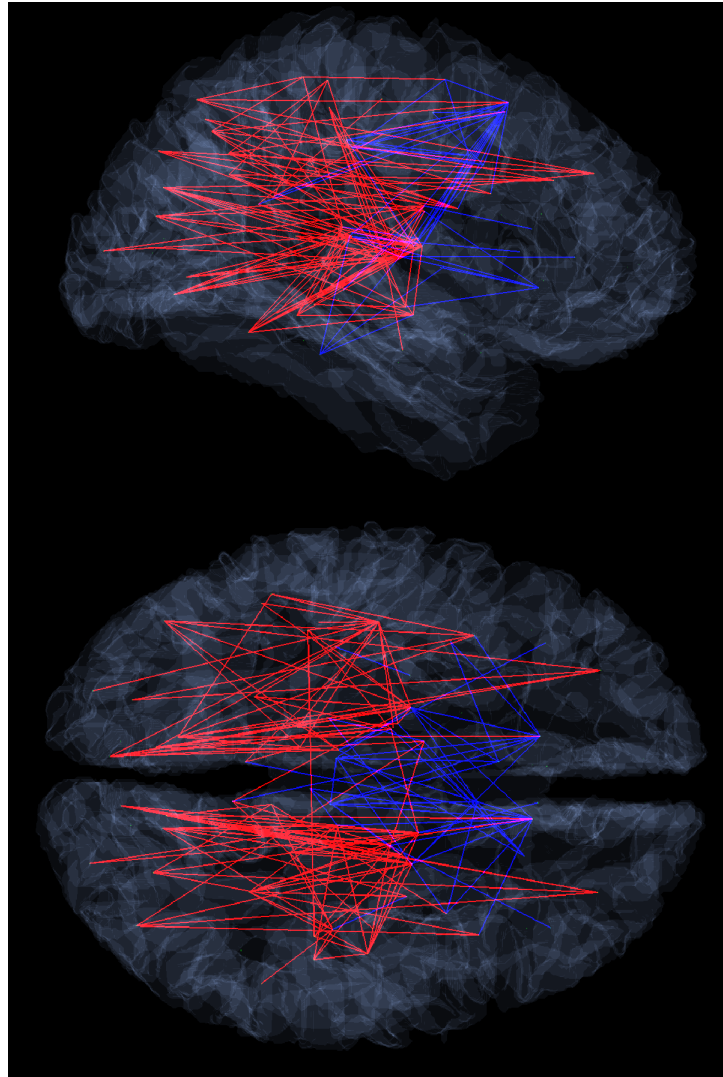


Figure 1: Location of the 158 significant sex-implicator edges with the fiber number (fn) weighting in sagittal and horizontal positions. In red edges, the fiber number is significantly larger in women (they are the female impicator edges). In blue edges, the fiber number is significantly larger in men (they are the male impicator edges). The upper panel shows the brain in the sagittal, the lower panel in the horizontal position. It is very surprising to notice that the blue male impicator edges are more frequent in the anterior parts of the brain, while the red female impicator edges in the posterior lobes.

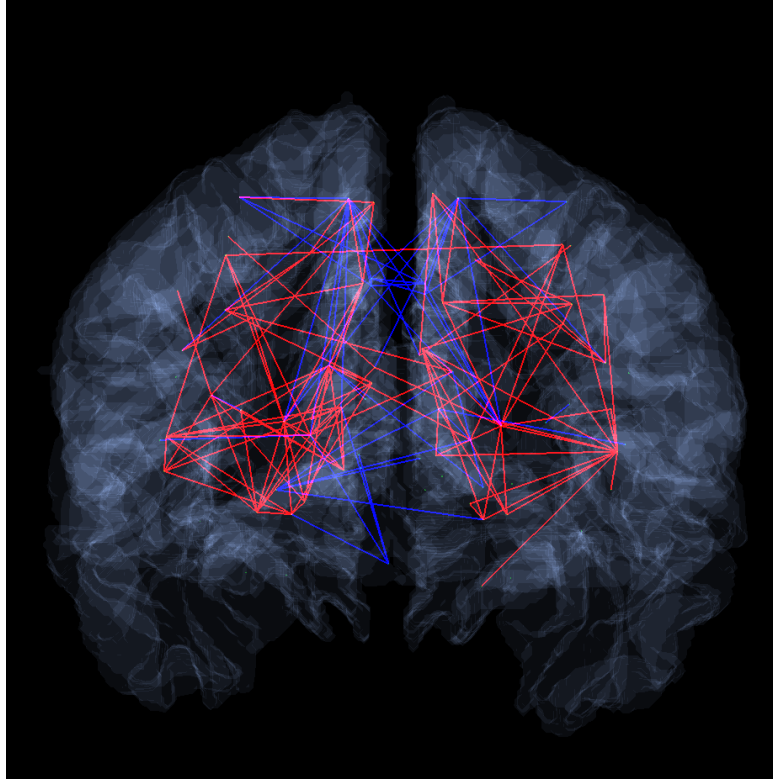


Figure 2: Location of the 158 significant sex-implicator edges with the fiber number (fn) weighting in coronal view. Red edges are the female impicator edges; blue edges are the male impicator edges. One should observe that the inter-hemispheric impicator edges are mostly blue, while the red, female impicator edges are mostly intra-hemispheric ones.

For the first view, the findings of Figure 2 are in contrast to the results of [37], which stated that the inter-hemispheric connections of males are weaker than females. However, our findings here do not necessarily contradict with [37]: we do not count the inter-hemispheric and intra-hemispheric connections here, but rather have identified the sex-implicator connections with different weight functions; that is, our method, focus, and analysis are quite distinct from that of [37].

Results with weight functions con , fa , and fl

The tables in the on-line supporting material (Tables S3, S4, and S5) list the edges, implying the male or female sex with cut-values determined in con , fa and fl weight functions, respectively. The supporting Figures S2, S3, and S4 visualize the significant sex impicator edges, using these weight functions. Additionally, supporting animations are available for visualizing the impicator edges with fiber number (fn) weight <https://youtu.be/VHVPghr8Ms4>, with fiber length (fl) weight <https://youtu.be/KVzP50pxU2E>, with fractional anisotropy (fa) weight <https://youtu.be/-bkB2qqXawY>, and conductivity (con) weight <https://youtu.be/oQF03QLuCNY>.

Table S5 and Figure S4 with the fiber-length weight function have some surprising edges: anatomically, the brains of men are larger than the brains of women by around 7% in volume [38]; therefore, it is natural that most sex impicator edges for males are corresponding to longer brain connections. In other words, in Figure S4, most impicator edges are colored blue. That is, they imply male subjects if longer than a cut-value.

However, some edges are red, meaning that even in the fiber length (fl) weight function, their longer lengths imply female subjects.

The edges connecting the parsopercularis and precentral areas in both left and right hemispheres are implying the female sex if they are longer, as well as the edge between the putamen and hippocampus, both in the right and left hemispheres (Table S5). These findings are in line with the results of [39], where differences in developmental trajectories of sexes were observed in these areas. Here we first proved that the length of these edges has very strong and implicative sex differences with longer lengths in females.

We note that our quantitative findings with cut-values and accuracy measures make our method applicable in diffusion MRI-based diagnostic tools for neurodegenerative- and psychiatric diseases if high-quality and large MRI datasets would become available for the public.

Age implicator edges

We attempted to apply the previous method on the property of age instead of sex. Probably since the age span of the subjects is not large enough (from 1064 subjects, 224 were between 21 and 25 years; 466 between 26 and 30 years; 364 between 31 and 36; and 10 were older than 36), we achieved only a moderate success.

We were interested in the difference between the 21-25 age group (“young”) and the 31-35 age group (“old”), so we also selected 224 subjects from the “old” group and compared them with the “young” subjects.

Because of the small number of examples and probably less difference between classes, controlling FWER was not possible, so we have controlled the false discovery rate (FDR) instead of FWER. Given m number of hypotheses, if the number of discoveries (rejections of hypotheses) is R , and the number of false discoveries is V , then $\text{FDR} = E(\frac{V}{R})$. Thus an upper bound $\text{FDR} < \alpha$ would tell that the expected rate of false discoveries does not exceed α .

In bioinformatics, an upper bound on FDR is still valuable because if the number of rejections is small, then checking these hypotheses experimentally probably reveals the feature of interest (e.g., in gene expression data).

Benjamini and Yekutieli provided a general procedure for controlling FDR with α in cases of arbitrary dependencies [40]. The recipe is as follows: (i) Sort the p-values: $p_1 \leq \dots \leq p_m$; (ii) Find the largest k for $p_k \leq \frac{k}{mc(m)}\alpha$, where $c(m) = \sum_{i=1}^m \frac{1}{i}$. (iii) Reject the first k hypotheses.

Table 2 shows the results.

Vertex 1	Vertex 2	Young ? Old	c	p_ks	D_ks	ACC	ACC_ks	FDR
1 rh.paracentral	Right-Pallidum	Y>O	41	4e-06	0.24	0.62	0.62	0.06
2 lh.parsopercularis	lh.inferiorparietal	Y<O	4	3e-05	0.22	0.61	0.61	0.21
3 rh.paracentral	Right-Thalamus-Proper	Y>O	94	6e-05	0.21	0.61	0.61	0.34
4 rh.paracentral	Right-Putamen	Y>O	306	6e-05	0.21	0.61	0.61	0.26
5 lh.insula	Left-Pallidum	Y>O	230	6e-05	0.21	0.61	0.61	0.20
6 lh.caudalanteriorcingulate	Left-Caudate	Y>O	2903	6e-05	0.21	0.61	0.61	0.17
7 rh.caudalmiddlefrontal	Right-Thalamus-Proper	Y>O	552	2e-04	0.21	0.60	0.60	0.34
8 rh.postcentral	Right-Pallidum	Y>O	37	2e-04	0.21	0.60	0.60	0.30
9 rh.caudalanteriorcingulate	rh.insula	Y>O	144	2e-04	0.20	0.60	0.60	0.40
10 rh.precentral	rh.precuneus	Y<O	54	2e-04	0.20	0.60	0.60	0.36

Table 2: The ten most significant edges with the *fn* weight function in age. The index column refers to the ranking, *Vertex 1* and *Vertex 2* are the corresponding brain areas connected by the edge, $Y>O$ indicates an edge where the “young” implication is valid if the weight of the edge is larger than the “ c ” cut-value, while $Y<O$ indicates an edge where the “old” implication is valid if the weight of the edge is larger than the “ c ” cut-value. The p_ks and D_ks mean the Kolmogorov-Smirnov p-value and statistics for an edge. ACC denotes the accuracy of the implication, ACC_ks denotes the $\frac{1}{2}(1 + D_ks)$ Kolmogorov-Smirnov estimation for best separation accuracy. FDR is the Benjamini-Yekutieli upper bound for the false discovery rate. Table S2 in the supporting material contains the whole result-set.

For example, if we set $\alpha = 0.17$, then the first 6 edges could be called significant with the assumption that the number of false discoveries would be ≤ 1.02 . Here the ACC and ACC_ks are the same; each class contains the same number (= 224) of elements.

Conclusions

We have demonstrated that certain *single* brain connections can be applied for inferring biological properties of the subjects with strict statistical validity. We have shown that the fiber number, the fiber length, the fractional anisotropy, and a connectivity-related edge-weight of specific edges can be applied for predicting the sex and the age of the subjects with 67% and 62% accuracy, respectively. To our knowledge, this is the first result, which uses the properties of single braingraph edges for gaining statistically valid biological implications. Our method is believed to be applicable in other implications besides age or sex if high-quality diffusion MRI datasets become available.

Apart from the possible diagnostic use, the impicator edges are the most important ones in distinguishing the biological properties examined. This way, we have demonstrated the most important single connections related to specific biological properties in large graphs.

Author contributions:

LK and ES suggested using the statistical methods for the identification of single edges with the implications described in this work, contributed statistical methods and analyzed the results. BV computed the braingraphs from the HCP public data and prepared the figures and the supplementary videos accompanying the present work. VG initiated the study, secured funding, analyzed the results, and wrote the paper.

Data availability

The data source of this work was published at the Human Connectome Project’s website at <http://www.humanconnectome.org> [27] as the 1200-subjects public release. The parcellation data, containing the anatomically labeled ROIs, is listed in the CMTK nipyipe GitHub repository https://github.com/LTS5/cmp_nipyipe/blob/master/cmtklib/data/parcellation/lausanne2008/ParcellationLausanne2008.xls. The underlying braingraph set is published and downloadable at <https://braingraph.org>, with the methodology described in detail in [26]. The supporting animations for visualizing the impicator edges with fiber number (*fn*) weight is available at <https://youtu.be/VHPgthr8Ms4>, with fiber length (*fl*) weight at <https://youtu.be/KVzP50pxU2E>, with fractional anisotropy (*fa*) weight at <https://youtu.be/-bkB2qqXawY>, and conductivity (*con*) weight at <https://youtu.be/oQF03QLuCNY>.

Acknowledgments

Data were provided in part by the Human Connectome Project, WU-Minn Consortium (Principal Investigators: David Van Essen and Kamil Ugurbil; 1U54MH091657) funded by the 16 NIH Institutes and Centers that support the NIH Blueprint for Neuroscience Research; and by the McDonnell Center for Systems Neuroscience at Washington University. VG and BV were partially supported by the VEKOP-2.3.2-16-2017-00014 program, supported by the European Union and the State of Hungary, co-financed by the European Regional Development Fund, VG by NKFI-127909 grants of the National Research, Development and Innovation Office of Hungary. LK and ES were supported in part by the EFOP-3.6.3-VEKOP-16-2017-00002 grant, supported by the European Union, co-financed by the European Social Fund.

References

- [1] K C Nicolaou. Advancing the drug discovery and development process. *Angewandte Chemie (International ed. in English)*, 53:9128–9140, August 2014.
- [2] Patric Hagmann, Patricia E. Grant, and Damien A. Fair. MR connectomics: a conceptual framework for studying the developing brain. *Front Syst Neurosci*, 6:43, 2012.
- [3] D. C. Van Essen, K. Ugurbil, E. Auerbach, D. Barch, T E J. Behrens, R. Bucholz, A. Chang, L. Chen, M. Corbetta, S. W. Curtiss, S. Della Penna, D. Feinberg, M. F. Glasser, N. Harel, A. C. Heath, L. Larson-Prior, D. Marcus, G. Michalareas, S. Moeller, R. Oostenveld, S. E. Petersen, F. Prior, B. L. Schlaggar, S. M. Smith, A. Z. Snyder, J. Xu, E. Yacoub, and W. U-Minn H. C. P Consortium . The human connectome project: a data acquisition perspective. *Neuroimage*, 62(4):2222–2231, Oct 2012.
- [4] Olaf Sporns, Giulio Tononi, and Rolf Kötter. The human connectome: A structural description of the human brain. *PLoS Computational Biology*, 1(4):e42, Sep 2005.
- [5] Alessandro Daducci, Stephan Gerhard, Alessandra Griffa, Alia Lemkadem, Leila Cammoun, Xavier Gigandet, Reto Meuli, Patric Hagmann, and Jean-Philippe Thiran. The connectome mapper: an open-source processing pipeline to map connectomes with MRI. *PLoS One*, 7(12):e48121, 2012.
- [6] Bruce Fischl. Freesurfer. *Neuroimage*, 62(2):774–781, 2012.
- [7] Csaba Kerepesi, Balazs Szalkai, Balint Varga, and Vince Grolmusz. The braingraph. org database of high resolution structural connectomes and the brain graph tools. *Cognitive Neurodynamics*, 11(5):483–486, 2017.
- [8] Csaba Kerepesi, Balazs Szalkai, Balint Varga, and Vince Grolmusz. How to direct the edges of the connectomes: Dynamics of the consensus connectomes and the development of the connections in the human brain. *PLOS One*, 11(6):e0158680, June 2016.
- [9] Balazs Szalkai, Csaba Kerepesi, Balint Varga, and Vince Grolmusz. High-resolution directed human connectomes and the consensus connectome dynamics. *PLoS ONE*, 14(4), September 2019.
- [10] F Thomson Leighton. *Introduction to parallel algorithms and architectures: Arrays, trees, hypercubes*. Elsevier, 1992.
- [11] Balázs Szalkai, Bálint Varga, and Vince Grolmusz. Graph theoretical analysis reveals: Women’s brains are better connected than men’s. *PLoS One*, 10(7):e0130045, 2015.
- [12] Balázs Szalkai, Bálint Varga, and Vince Grolmusz. The graph of our mind. *Brain Sciences*, 11(3), 2021.
- [13] Balazs Szalkai, Balint Varga, and Vince Grolmusz. Comparing advanced graph-theoretical parameters of the connectomes of the lobes of the human brain. *Cognitive Neurodynamics*, 12(6):549–559, 2018.
- [14] Balazs Szalkai, Balint Varga, and Vince Grolmusz. Mapping correlations of psychological and connectomical properties of the dataset of the human connectome project with the maximum spanning tree method. *Brain Imaging and Behavior*, 13(5):1185–1192, feb 2019.
- [15] Balázs Szalkai, Bálint Varga, and Vince Grolmusz. Brain size bias-compensated graph-theoretical parameters are also better in women’s connectomes. *Brain Imaging and Behavior*, 12(3):663–673, 2018.

- [16] William James Dally and Brian Towles. *Principles and practices of interconnection networks*. Elsevier, Morgan Kaufmann, 2007. Includes bibliographical references and index.
- [17] Balázs Szalkai, Csaba Kerepesi, Bálint Varga, and Vince Grolmusz. The Budapest Reference Connectome Server v2. 0. *Neuroscience Letters*, 595:60–62, 2015.
- [18] Balazs Szalkai, Csaba Kerepesi, Balint Varga, and Vince Grolmusz. Parameterizable consensus connectomes from the Human Connectome Project: The Budapest Reference Connectome Server v3.0. *Cognitive Neurodynamics*, 11(1):113–116, feb 2017.
- [19] Csaba Kerepesi, Balázs Szalkai, Bálint Varga, and Vince Grolmusz. Comparative connectomics: Mapping the inter-individual variability of connections within the regions of the human brain. *Neuroscience Letters*, 662(1):17–21, 2018.
- [20] Mate Fellner, Balint Varga, and Vince Grolmusz. The frequent subgraphs of the connectome of the human brain. *Cognitive Neurodynamics*, 13(5):453–460, 2019.
- [21] Máté Fellner, Bálint Varga, and Vince Grolmusz. The frequent complete subgraphs in the human connectome. *PloS One*, 15(8):e0236883, 2020.
- [22] Mate Fellner, Balint Varga, and Vince Grolmusz. The frequent network neighborhood mapping of the human hippocampus shows much more frequent neighbor sets in males than in females. *PLOS One*, 15(1):e0227910, 2020.
- [23] Mate Fellner, Balint Varga, and Vince Grolmusz. Good neighbors, bad neighbors: The frequent network neighborhood mapping of the hippocampus enlightens several structural factors of the human intelligence on a 414-subject cohort. *Scientific Reports*, 10(11967), 2020.
- [24] Laszlo Keresztes, Evelin Szogi, Balint Varga, and Vince Grolmusz. Identifying super-feminine, super-masculine and sex-defining connections in the human braingraph. *Cognitive Neurodynamics, to appear*, 2021.
- [25] David C. Van Essen, Stephen M. Smith, Deanna M. Barch, Timothy E J. Behrens, Essa Yacoub, Kamil Ugurbil, and W. U-Minn H. C. P Consortium . The wu-minn human connectome project: an overview. *Neuroimage*, 80:62–79, Oct 2013.
- [26] Balint Varga and Vince Grolmusz. The braingraph.org database with more than 1000 robust human structural connectomes in five resolutions. *Cognitive Neurodynamics*, 2021.
- [27] Jennifer A. McNab, Brian L. Edlow, Thomas Witzel, Susie Y. Huang, Himanshu Bhat, Keith Heberlein, Thorsten Feiweier, Kecheng Liu, Boris Keil, Julien Cohen-Adad, M Dylan Tisdall, Rebecca D. Folkerth, Hannah C. Kinney, and Lawrence L. Wald. The Human Connectome Project and beyond: initial applications of 300 mT/m gradients. *Neuroimage*, 80:234–245, Oct 2013.
- [28] J Tournier, Fernando Calamante, Alan Connelly, et al. Mrtrix: diffusion tractography in crossing fiber regions. *International Journal of Imaging Systems and Technology*, 22(1):53–66, 2012.
- [29] Peter J. Basser and Carlo Pierpaoli. Microstructural and physiological features of tissues elucidated by quantitative-diffusion-tensor mri. *J Magn Reson*, 213(2):560–570, Dec 1996.
- [30] Frank J. Massey Jr. The Kolmogorov-Smirnov test for goodness of fit. *Journal of the American Statistical Association*, 46(253):68–78, 1951.

- [31] Pauli Virtanen, Ralf Gommers, Travis E. Oliphant, Matt Haberland, Tyler Reddy, David Cournapeau, Evgeni Burovski, Pearu Peterson, Warren Weckesser, Jonathan Bright, Stéfan J. van der Walt, Matthew Brett, Joshua Wilson, K. Jarrod Millman, Nikolay Mayorov, Andrew R. J. Nelson, Eric Jones, Robert Kern, Eric Larson, C J Carey, İlhan Polat, Yu Feng, Eric W. Moore, Jake VanderPlas, Denis Laxalde, Josef Perktold, Robert Cimrman, Ian Henriksen, E. A. Quintero, Charles R. Harris, Anne M. Archibald, Antônio H. Ribeiro, Fabian Pedregosa, Paul van Mulbregt, and SciPy 1.0 Contributors. SciPy 1.0: Fundamental Algorithms for Scientific Computing in Python. *Nature Methods*, 17:261–272, 2020.
- [32] Sture Holm. A simple sequentially rejective multiple test procedure. *Scandinavian Journal of Statistics*, 6(2):65–70, 1979.
- [33] Mark Rijpkema, Daphne Everaerd, Carline van der Pol, Barbara Franke, Indira Tendolkar, and Guillén Fernández. Normal sexual dimorphism in the human basal ganglia. *Human brain mapping*, 33:1246–1252, May 2012.
- [34] A Veronica Witte, Markus Savli, Alexander Holik, Siegfried Kasper, and Rupert Lanzenberger. Regional sex differences in grey matter volume are associated with sex hormones in the young adult human brain. *Neuroimage*, 49(2):1205–1212, 2010.
- [35] J. N. Giedd, F. X. Castellanos, J. C. Rajapakse, A. C. Vaituzis, and J. L. Rapoport. Sexual dimorphism of the developing human brain. *Progress in neuro-psychopharmacology & biological psychiatry*, 21:1185–1201, November 1997.
- [36] M. E. Frederikse, A. Lu, E. Aylward, P. Barta, and G. Pearlson. Sex differences in the inferior parietal lobule. *Cerebral cortex (New York, N.Y. : 1991)*, 9:896–901, December 1999.
- [37] Madhura Ingalkar, Alex Smith, Drew Parker, Theodore D. Satterthwaite, Mark A. Elliott, Kosha Ruparel, Hakon Hakonarson, Raquel E. Gur, Ruben C. Gur, and Ragini Verma. Sex differences in the structural connectome of the human brain. *Proc Natl Acad Sci U S A*, 111(2):823–828, Jan 2014.
- [38] S. F. Witelson, H. Beresh, and D. L. Kigar. Intelligence and brain size in 100 postmortem brains: sex, lateralization and age factors. *Brain*, 129(2):386–398, Feb 2006.
- [39] Anne-Lise Goddings, Kathryn L. Mills, Liv S. Clasen, Jay N. Giedd, Russell M. Viner, and Sarah-Jayne Blakemore. The influence of puberty on subcortical brain development. *NeuroImage*, 88:242–251, March 2014.
- [40] Yoav Benjamini and Daniel Yekutieli. The control of the false discovery rate in multiple testing under dependency. *Annals of Statistics*, 29(4):1165–1188, 2001.

Supporting Material

Results with the fiber number (fn) weight function

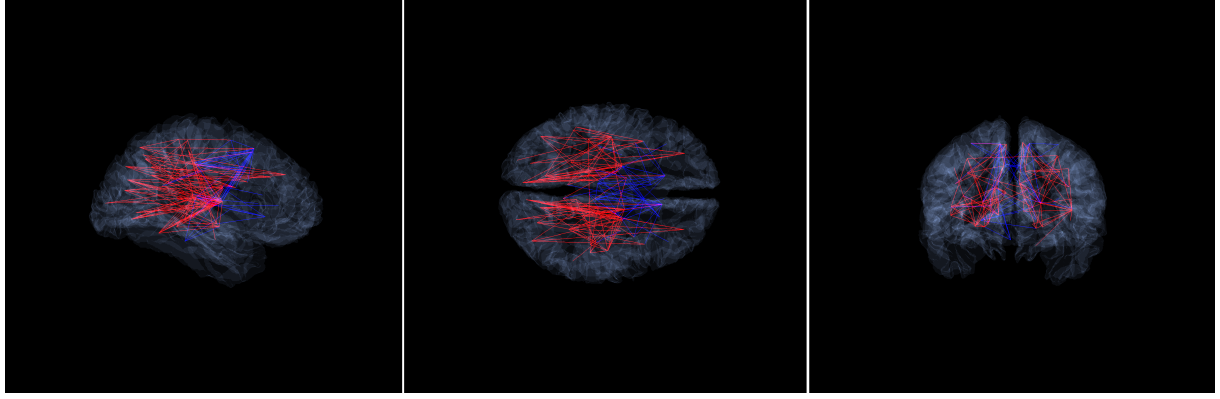


Figure S1. Sex impicator edges with the fiber number (fn) weight function. Red color denotes edges where the higher fiber number implies the female sex, while blue edges correspond to those where the higher fiber number implies the male sex (cf. with Table S1). Three views correspond (from left to right) to sagittal, horizontal, and coronal positions. One may observe that red edges are mostly located in the posterior, while blue edges in the anterior lobes. Additionally, the inter-hemispheric edges are mostly blue ones. An animation of these images is available at <https://youtu.be/VHPg8Ms4>.

Table S1: Sex impicator edges with the fiber number (fn) weight function

The row index shows the ranking, *Vertex 1* and *Vertex 2* are the corresponding brain areas, connected by the edge, $M>F$ indicates an edge with weight function significantly higher in males, while $M<F$ indicates an edge with weight function significantly higher in females. The p_{-ks} and D_{-ks} mean the Kolmogorov-Smirnov p-value and statistics for an edge. *ACC* denotes the accuracy of the best separation, *ACC_ks* denotes the $\frac{1}{2}(1 + D_{-ks})$ Kolmogorov-Smirnov estimation for best separation accuracy. *FWER* in the k th row shows the Family-Wise Error Rate upper bound for the first k edges.

Vertex 1	Vertex 2	Male ?	Female	p_{-ks}	D_{-ks}	ACC	ACC_{-ks}	FWER
1 lh.superiorparietal	Left-Caudate	M<F		1e-30	0.36	0.67	0.68	2e-27
2 lh.rostralmiddlefrontal	Left-Caudate	M>F		8e-29	0.35	0.67	0.67	1e-25
3 rh.caudalanteriorcingulate	lh.rostralmiddlefrontal	M>F		4e-28	0.34	0.67	0.67	8e-25
4 lh.precuneus	Left-Caudate	M<F		4e-27	0.34	0.67	0.67	9e-24
5 lh.parsopercularis	lh.inferiorparietal	M<F		8e-27	0.33	0.67	0.67	2e-23
6 rh.rostralmiddlefrontal	Right-Caudate	M>F		5e-25	0.32	0.67	0.66	9e-22
7 rh.precuneus	Right-Caudate	M<F		1e-24	0.32	0.66	0.66	2e-21
8 rh.rostralanteriorcingulate	rh.caudalanteriorcingulate	M>F		2e-24	0.32	0.66	0.66	3e-21
9 rh.caudalanteriorcingulate	Right-Caudate	M>F		3e-24	0.32	0.66	0.66	6e-21
10 lh.rostralanteriorcingulate	lh.caudalanteriorcingulate	M>F		4e-24	0.32	0.66	0.66	8e-21
11 rh.parsopercularis	rh.inferiorparietal	M<F		5e-24	0.32	0.65	0.66	1e-20
12 Right-Putamen	Right-Amygdala	M>F		6e-22	0.30	0.65	0.65	1e-18
13 rh.superiortemporal	rh.transversetemporal	M>F		1e-21	0.30	0.65	0.65	3e-18
14 Right-Caudate	lh.rostralmiddlefrontal	M>F		7e-21	0.30	0.64	0.65	1e-17
15 rh.precuneus	Right-Hippocampus	M<F		2e-20	0.29	0.64	0.65	4e-17
16 rh.precuneus	Right-Putamen	M<F		2e-20	0.29	0.65	0.65	4e-17
17 rh.superiorparietal	Right-Caudate	M<F		2e-20	0.29	0.65	0.65	4e-17

18	lh.posteriorcingulate	Left-Putamen	M<F	3e-20	0.29	0.64	0.65	5e-17
19	lh.parsopercularis	lh.supramarginal	M<F	5e-20	0.29	0.64	0.64	9e-17
20	Left-Putamen	Left-Amygdala	M>F	6e-20	0.29	0.65	0.64	1e-16
21	rh.insula	Right-Amygdala	M>F	6e-19	0.28	0.64	0.64	1e-15
22	lh.fusiform	Left-Hippocampus	M<F	7e-19	0.28	0.64	0.64	1e-15
23	lh.inferiorparietal	Left-Thalamus-Proper	M<F	2e-18	0.28	0.64	0.64	3e-15
24	lh.lingual	Left-Putamen	M<F	6e-18	0.27	0.63	0.64	1e-14
25	rh.rostralanteriorcingulate	Right-Caudate	M>F	8e-18	0.27	0.64	0.64	1e-14
26	Right-Accumbens-area	Left-Thalamus-Proper	M>F	4e-17	0.27	0.64	0.63	7e-14
27	lh.inferiorparietal	Left-Putamen	M<F	1e-16	0.26	0.63	0.63	3e-13
28	rh.parsopercularis	rh.supramarginal	M<F	2e-16	0.26	0.63	0.63	4e-13
29	lh.parstriangularis	lh.rostralmiddlefrontal	M>F	2e-16	0.26	0.63	0.63	4e-13
30	lh.bankssts	Left-Hippocampus	M<F	2e-16	0.26	0.64	0.63	5e-13
31	lh.inferiorparietal	Left-Caudate	M<F	3e-16	0.26	0.63	0.63	6e-13
32	rh.rostralmiddlefrontal	lh.caudalanteriorcingulate	M>F	4e-16	0.26	0.63	0.63	7e-13
33	lh.parsopercularis	lh.superiorparietal	M<F	3e-15	0.25	0.63	0.63	7e-12
34	rh.pericalcarine	rh.bankssts	M<F	3e-15	0.25	0.63	0.63	7e-12
35	lh.bankssts	Left-Caudate	M<F	3e-15	0.26	0.63	0.63	7e-12
36	rh.parstriangularis	rh.supramarginal	M<F	4e-15	0.25	0.62	0.62	9e-12
37	lh.isthmuscingulate	Left-Caudate	M<F	8e-15	0.25	0.63	0.62	2e-11
38	Right-Caudate	lh.rostralanteriorcingulate	M>F	8e-15	0.25	0.64	0.62	2e-11
39	lh.superiorfrontal	lh.rostralanteriorcingulate	M>F	8e-15	0.25	0.61	0.62	2e-11
40	rh.superiorfrontal	rh.rostralanteriorcingulate	M>F	1e-14	0.25	0.62	0.62	2e-11
41	lh.lateraloccipital	Left-Thalamus-Proper	M<F	1e-14	0.25	0.62	0.62	2e-11
42	rh.lingual	Right-Putamen	M<F	2e-14	0.25	0.62	0.62	3e-11
43	Left-Pallidum	Left-Amygdala	M>F	2e-14	0.25	0.63	0.62	3e-11
44	rh.precentral	rh.inferiorparietal	M<F	2e-14	0.24	0.62	0.62	4e-11
45	lh.rostralmiddlefrontal	lh.superiorfrontal	M>F	2e-14	0.24	0.62	0.62	5e-11
46	lh.lingual	lh.insula	M<F	3e-14	0.24	0.62	0.62	7e-11
47	lh.inferiortemporal	Left-Hippocampus	M<F	4e-14	0.24	0.62	0.62	9e-11
48	lh.rostralmiddlefrontal	lh.caudalanteriorcingulate	M>F	5e-14	0.24	0.62	0.62	9e-11
49	rh.insula	Right-Putamen	M>F	5e-14	0.24	0.62	0.62	9e-11
50	rh.lingual	rh.bankssts	M<F	7e-14	0.24	0.63	0.62	1e-10
51	rh.inferiorparietal	Right-Caudate	M<F	8e-14	0.24	0.62	0.62	2e-10
52	lh.isthmuscingulate	lh.bankssts	M<F	8e-14	0.24	0.62	0.62	2e-10
53	rh.bankssts	Right-Caudate	M<F	1e-13	0.24	0.62	0.62	2e-10
54	lh.postcentral	lh.superiortemporal	M<F	1e-13	0.24	0.61	0.62	3e-10
55	lh.precuneus	Left-Putamen	M<F	2e-13	0.24	0.62	0.62	3e-10
56	Left-Caudate	Left-Hippocampus	M<F	2e-13	0.24	0.63	0.62	4e-10
57	rh.postcentral	rh.bankssts	M<F	3e-13	0.24	0.60	0.62	5e-10
58	rh.isthmuscingulate	Right-Putamen	M<F	3e-13	0.23	0.62	0.62	5e-10
59	rh.fusiform	rh.bankssts	M<F	3e-13	0.23	0.63	0.62	6e-10
60	rh.parsopercularis	rh.precuneus	M<F	3e-13	0.23	0.61	0.62	6e-10
61	rh.rostralmiddlefrontal	rh.inferiorparietal	M<F	3e-13	0.23	0.61	0.62	7e-10
62	lh.precentral	lh.supramarginal	M<F	4e-13	0.23	0.61	0.62	7e-10
63	rh.rostralanteriorcingulate	lh.caudalanteriorcingulate	M>F	5e-13	0.23	0.63	0.62	1e-09
64	rh.isthmuscingulate	Right-Caudate	M<F	8e-13	0.23	0.62	0.62	2e-09
65	lh.lateraloccipital	lh.insula	M<F	1e-12	0.23	0.62	0.61	2e-09
66	rh.precentral	rh.posteriorcingulate	M<F	1e-12	0.23	0.61	0.61	2e-09
67	lh.rostralmiddlefrontal	lh.insula	M>F	1e-12	0.23	0.63	0.61	2e-09
68	Left-Caudate	Left-Putamen	M<F	1e-12	0.23	0.61	0.61	2e-09
69	lh.precentral	lh.inferiorparietal	M<F	1e-12	0.23	0.62	0.61	2e-09
70	rh.rostralmiddlefrontal	Left-Caudate	M>F	2e-12	0.23	0.61	0.61	3e-09
71	lh.parstriangularis	lh.supramarginal	M<F	2e-12	0.23	0.59	0.61	4e-09
72	lh.bankssts	Left-Putamen	M<F	2e-12	0.23	0.61	0.61	5e-09
73	lh.inferiortemporal	lh.bankssts	M<F	2e-12	0.23	0.61	0.61	5e-09

74	rh.inferior temporal	rh.bankssts	M < F	2e-12	0.23	0.61	0.61	5e-09
75	Right-Thalamus-Proper	Right-Accumbens-area	M > F	3e-12	0.23	0.62	0.61	5e-09
76	rh.caudal anterior cingulate	lh.superior frontal	M > F	3e-12	0.23	0.62	0.61	6e-09
77	Right-Caudate	lh.posterior cingulate	M < F	4e-12	0.22	0.61	0.61	7e-09
78	lh.caudal middle frontal	lh.posterior cingulate	M < F	4e-12	0.22	0.62	0.61	8e-09
79	lh.lingual	Left-Thalamus-Proper	M < F	6e-12	0.22	0.62	0.61	1e-08
80	lh.isthmus cingulate	Left-Putamen	M < F	7e-12	0.22	0.62	0.61	1e-08
81	rh.caudal middle frontal	rh.posterior cingulate	M < F	7e-12	0.22	0.62	0.61	1e-08
82	rh.rostral middle frontal	rh.superior frontal	M > F	8e-12	0.22	0.60	0.61	1e-08
83	lh.bankssts	Left-Thalamus-Proper	M < F	8e-12	0.22	0.61	0.61	2e-08
84	rh.fusiform	Right-Hippocampus	M < F	8e-12	0.22	0.60	0.61	2e-08
85	rh.lateral occipital	rh.bankssts	M < F	9e-12	0.22	0.61	0.61	2e-08
86	Right-Thalamus-Proper	Left-Putamen	M < F	9e-12	0.22	0.60	0.61	2e-08
87	rh.superior parietal	rh.insula	M < F	1e-11	0.22	0.61	0.61	2e-08
88	lh.pericalcarine	Left-Thalamus-Proper	M < F	1e-11	0.22	0.61	0.61	2e-08
89	lh.pars opercularis	lh.precuneus	M < F	1e-11	0.22	0.60	0.61	2e-08
90	lh.fusiform	lh.insula	M < F	2e-11	0.22	0.61	0.61	3e-08
91	rh.parstriangularis	rh.superior parietal	M < F	2e-11	0.22	0.59	0.61	4e-08
92	lh.lingual	Left-Caudate	M < F	3e-11	0.22	0.61	0.61	5e-08
93	lh.bankssts	lh.insula	M < F	3e-11	0.22	0.61	0.61	7e-08
94	lh.pericalcarine	lh.insula	M < F	4e-11	0.21	0.60	0.61	7e-08
95	lh.precuneus	Left-Thalamus-Proper	M < F	4e-11	0.21	0.61	0.61	7e-08
96	rh.precuneus	Right-Thalamus-Proper	M < F	4e-11	0.21	0.61	0.61	8e-08
97	rh.caudal anterior cingulate	lh.rostral anterior cingulate	M > F	7e-11	0.21	0.62	0.61	1e-07
98	Right-Pallidum	Right-Amygdala	M > F	7e-11	0.21	0.60	0.61	1e-07
99	lh.lateral occipital	Left-Caudate	M < F	8e-11	0.21	0.60	0.61	1e-07
100	lh.lateral occipital	Left-Putamen	M < F	8e-11	0.21	0.60	0.61	2e-07
101	lh.insula	Left-Amygdala	M > F	9e-11	0.21	0.61	0.61	2e-07
102	rh.lateral occipital	Right-Putamen	M < F	9e-11	0.21	0.59	0.61	2e-07
103	rh.bankssts	Right-Hippocampus	M < F	1e-10	0.21	0.60	0.61	2e-07
104	rh.pars opercularis	rh.superior parietal	M < F	1e-10	0.21	0.60	0.61	2e-07
105	rh.lingual	rh.insula	M < F	1e-10	0.21	0.60	0.61	2e-07
106	lh.lingual	Left-Hippocampus	M < F	1e-10	0.21	0.60	0.60	2e-07
107	lh.lingual	lh.superior temporal	M < F	1e-10	0.21	0.60	0.60	3e-07
108	rh.posterior cingulate	lh.rostral middle frontal	M > F	2e-10	0.21	0.61	0.60	3e-07
109	rh.lateral occipital	rh.insula	M < F	2e-10	0.21	0.59	0.60	4e-07
110	rh.precuneus	rh.bankssts	M < F	2e-10	0.21	0.61	0.60	5e-07
111	lh.precentral	lh.superior temporal	M < F	3e-10	0.21	0.58	0.60	6e-07
112	Right-Hippocampus	Right-Amygdala	M > F	3e-10	0.20	0.61	0.60	7e-07
113	rh.precentral	rh.superior parietal	M < F	3e-10	0.20	0.61	0.60	7e-07
114	rh.isthmus cingulate	lh.isthmus cingulate	M < F	4e-10	0.20	0.60	0.60	7e-07
115	rh.precuneus	rh.insula	M < F	4e-10	0.20	0.60	0.60	7e-07
116	lh.rostral anterior cingulate	Left-Caudate	M > F	4e-10	0.20	0.60	0.60	7e-07
117	lh.lingual	lh.bankssts	M < F	4e-10	0.20	0.61	0.60	8e-07
118	rh.postcentral	rh.inferior parietal	M < F	4e-10	0.20	0.60	0.60	8e-07
119	rh.parstriangularis	rh.postcentral	M < F	4e-10	0.20	0.60	0.60	8e-07
120	rh.rostral middle frontal	lh.posterior cingulate	M > F	5e-10	0.20	0.61	0.60	9e-07
121	lh.fusiform	lh.superior temporal	M < F	5e-10	0.20	0.61	0.60	1e-06
122	Right-Thalamus-Proper	Right-Amygdala	M > F	7e-10	0.20	0.59	0.60	1e-06
123	rh.parstriangularis	rh.rostral middle frontal	M > F	7e-10	0.20	0.61	0.60	1e-06
124	lh.inferior temporal	lh.insula	M < F	8e-10	0.20	0.60	0.60	1e-06
125	rh.precentral	rh.bankssts	M < F	8e-10	0.20	0.58	0.60	2e-06
126	lh.superior temporal	lh.transverse temporal	M > F	9e-10	0.20	0.61	0.60	2e-06
127	rh.parstriangularis	rh.inferior parietal	M < F	9e-10	0.20	0.57	0.60	2e-06
128	rh.middle temporal	rh.bankssts	M < F	9e-10	0.20	0.60	0.60	2e-06
129	lh.rostral middle frontal	Left-Thalamus-Proper	M > F	1e-09	0.20	0.61	0.60	2e-06

130	lh.rostralmiddlefrontal	Left-Putamen	M>F	1e-09	0.20	0.61	0.60	2e-06			
131	rh.lingual	Right-Caudate	M<F	1e-09	0.20	0.61	0.60	2e-06			
132	lh.lingual	lh.transversetemporal	M<F	1e-09	0.20	0.59	0.60	3e-06			
133	lh.superiorfrontal	lh.precentral	M<F	1e-09	0.20	0.59	0.60	3e-06			
134	lh.rostralmiddlefrontal	lh.supramarginal	M<F	1e-09	0.20	0.59	0.60	3e-06			
135	Right-Putamen	Left-Thalamus-Proper	M<F	2e-09	0.20	0.59	0.60	3e-06			
136	rh.lateraloccipital	Right-Caudate	M<F	2e-09	0.20	0.59	0.60	3e-06			
137	lh.parstriangularis	lh.superiorparietal	M<F	2e-09	0.20	0.58	0.60	4e-06			
138	lh.lateraloccipital	lh.superiortemporal	M<F	2e-09	0.20	0.60	0.60	4e-06			
139	lh.lateraloccipital	lh.transversetemporal	M<F	3e-09	0.19	0.60	0.60	6e-06			
140	lh.rostralmiddlefrontal	lh.inferiorparietal	M<F	3e-09	0.19	0.58	0.60	6e-06			
141	rh.lateralorbitofrontal	rh.insula	M>F	3e-09	0.19	0.60	0.60	6e-06			
142	rh.parahippocampal	rh.bankssts	M<F	3e-09	0.19	0.59	0.60	6e-06			
143	lh.inferiortemporal	Left-Thalamus-Proper	M<F	3e-09	0.19	0.60	0.60	6e-06			
144	lh.fusiform	Left-Caudate	M<F	3e-09	0.19	0.60	0.60	6e-06			
145	rh.middletemporal	Right-Caudate	M<F	3e-09	0.19	0.59	0.60	7e-06			
146	rh.isthmuscingulate	rh.bankssts	M<F	4e-09	0.19	0.60	0.60	7e-06			
147	lh.lateralorbitofrontal	Left-Putamen	M>F	4e-09	0.19	0.59	0.60	7e-06			
148	lh.rostralmiddlefrontal	lh.caudalanteriorcingulate	M>F	4e-09	0.19	0.60	0.60	8e-06			
149	rh.caudalanteriorcingulate	lh.caudalanteriorcingulate	M>F	4e-09	0.19	0.59	0.60	8e-06			
150	rh.rostralmiddlefrontal	rh.caudalanteriorcingulate	M>F	4e-09	0.19	0.59	0.60	8e-06			
151	rh.rostralmiddlefrontal	rh.rostralanteriorcingulate	M>F	6e-09	0.19	0.59	0.60	1e-05			
152	Right-Thalamus-Proper	lh.superiorparietal	M<F	7e-09	0.19	0.59	0.60	1e-05			
153	lh.inferiortemporal	lh.superiortemporal	M<F	7e-09	0.19	0.59	0.60	1e-05			
154	Right-Caudate	Right-Hippocampus	M<F	7e-09	0.19	0.59	0.60	1e-05			
155	lh.fusiform	Left-Thalamus-Proper	M<F	8e-09	0.19	0.60	0.60	1e-05			
156	lh.precuneus	Left-Hippocampus	M<F	8e-09	0.19	0.61	0.60	2e-05			
157	Left-Hippocampus	Left-Amygdala	M>F	1e-08	0.19	0.60	0.59	2e-05			
158	lh.paracentral	Left-Thalamus-Proper	M>F	1e-08	0.19	0.59	0.59	2e-05			

Table S2: Age impicator edges with the fiber number (fn) weight function

The row index shows the ranking, *Vertex 1* and *Vertex 2* are the corresponding brain areas, $Y > O$ indicates an edge where the “young” implication is valid if the weight of the edge is larger than the “ c ” cut-value, while $Y < O$ indicates an edge where the “old” implication is valid if the weight of the edge is larger than the “ c ” cut value. The p_{ks} and D_{ks} mean the Kolmogorov-Smirnov p-value and statistics for an edge. ACC denotes the accuracy of the best separation, ACC_{ks} denotes the $\frac{1}{2}(1 + D_{ks})$ Kolmogorov-Smirnov estimation for best separation accuracy. FDR is the Benjamini-Yekutieli upper bound to the false discovery rate.

	Vertex 1	Vertex 2	Young ? Old	c	p_ks	D_ks	ACC	ACC_ks	FDR
1	rh.paracentral	Right-Pallidum	Y>O	41	4e-06	0.24	0.62	0.62	0.06
2	lh.parsopercularis	lh.inferiorparietal	Y<O	4	3e-05	0.22	0.61	0.61	0.21
3	rh.paracentral	Right-Thalamus-Proper	Y>O	94	6e-05	0.21	0.61	0.61	0.34
4	rh.paracentral	Right-Putamen	Y>O	306	6e-05	0.21	0.61	0.61	0.26
5	lh.insula	Left-Pallidum	Y>O	230	6e-05	0.21	0.61	0.61	0.20
6	lh.caudalanteriorcingulate	Left-Caudate	Y>O	2903	6e-05	0.21	0.61	0.61	0.17
7	rh.caudalmiddlefrontal	Right-Thalamus-Proper	Y>O	552	2e-04	0.21	0.60	0.60	0.34
8	rh.postcentral	Right-Pallidum	Y>O	37	2e-04	0.21	0.60	0.60	0.30
9	rh.caudalanteriorcingulate	rh.insula	Y>O	144	2e-04	0.20	0.60	0.60	0.40
10	rh.precentral	rh.precuneus	Y<O	54	2e-04	0.20	0.60	0.60	0.36
11	lh.superiorfrontal	Left-Thalamus-Proper	Y>O	147	3e-04	0.20	0.60	0.60	0.49
12	rh.rostralmiddlefrontal	Right-Caudate	Y>O	1597	5e-04	0.19	0.60	0.60	0.67
13	rh.precentral	Right-Pallidum	Y>O	41	7e-04	0.19	0.59	0.59	0.90
14	rh.posteriorcingulate	rh.supramarginal	Y>O	426	7e-04	0.19	0.59	0.59	0.84

15	lh.rostralmiddlefrontal	lh.rostralanteriorcingulate	Y>O	72	7e-04	0.19	0.59	0.59	0.78
16	rh.precentral	Right-Thalamus-Proper	Y>O	387	7e-04	0.19	0.59	0.59	0.73
17	rh.caudalmiddlefrontal	Right-Pallidum	Y>O	77	7e-04	0.19	0.59	0.59	0.69
18	rh.precentral	rh.supramarginal	Y<O	2008	1e-03	0.18	0.59	0.59	0.95
19	lh.precentral	Left-Thalamus-Proper	Y>O	567	1e-03	0.18	0.59	0.59	0.90
20	rh.supramarginal	rh.superiortemporal	Y<O	40	1e-03	0.18	0.59	0.59	0.85

The conductivity (con) weight function

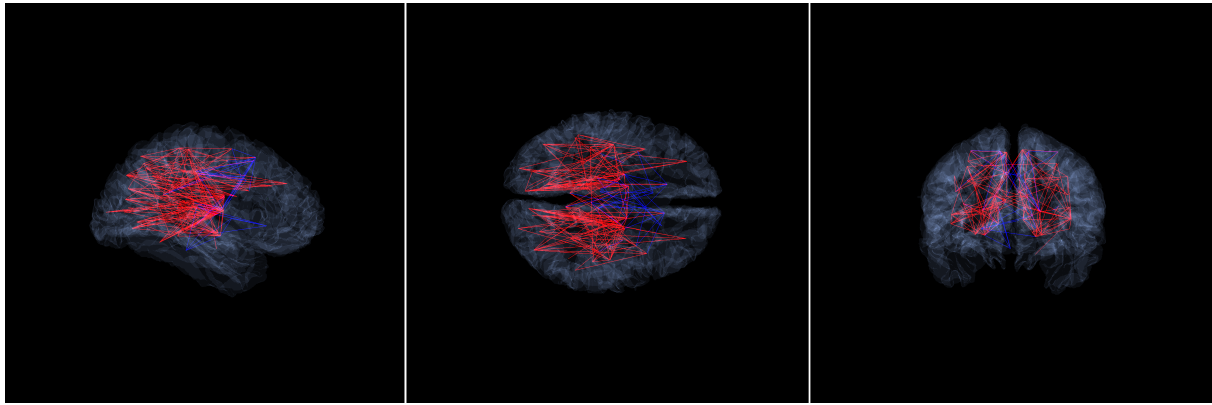


Figure S2. 193 sex impicator edges with the conductivity (con) weight function with $FWER < 1.95 \times 10^{-5}$. Red color denotes edges where the higher con weight implies the female sex, while blue edges correspond to those where higher con weight implies the male sex (cf. Table S3). Three views correspond (from left to right) to sagittal, horizontal, and coronal positions. One may observe that red edges are mostly located in the posterior, while blue edges in the anterior lobes. Additionally, the inter-hemispheric edges are mostly blue ones. An animation of these images is available at <https://youtu.be/oQF03QLuCNY>.

Table S3: Sex impicator edges with the conductivity (con) weight function

193 edges with $FWER < 1.95 \times 10^{-5}$ with the conductivity weight function. Index shows the ranking, *Vertex 1* and *Vertex 2* are the corresponding brain areas, $M>F$ indicates an edge with weight function significantly higher in males, while $M<F$ indicates an edge with weight function significantly higher in females. The p_{-ks} and D_{-ks} mean the Kolmogorov-Smirnov p-value and statistics for an edge. ACC denotes the accuracy of the best separation, ACC_{-ks} denotes the $\frac{1}{2}(1 + D_{-ks})$ KS estimation for best separation accuracy. $FWER$ in the k th row shows the FWER upper bound for the first k edges.

	Vertex 1	Vertex 2	Male ? Female	p_{-ks}	D_{-ks}	ACC	ACC_{-ks}	$FWER$
1	rh.precuneus	Right-Putamen	M<F	4e-30	0.35	0.68	0.68	8e-27
2	Right-Thalamus-Proper	Left-Thalamus-Proper	M<F	4e-30	0.35	0.68	0.68	8e-27
3	lh.inferiorparietal	Left-Thalamus-Proper	M<F	1e-28	0.35	0.67	0.67	2e-25
4	lh.precuneus	Left-Caudate	M<F	6e-28	0.34	0.66	0.67	1e-24
5	lh.parasubiculum	lh.inferiorparietal	M<F	3e-27	0.34	0.67	0.67	6e-24
6	rh.precuneus	Right-Caudate	M<F	1e-26	0.33	0.67	0.67	2e-23
7	lh.superiorparietal	Left-Caudate	M<F	1e-26	0.33	0.67	0.67	2e-23
8	rh.caudalanteriorcingulate	lh.rostralmiddlefrontal	M>F	5e-25	0.32	0.66	0.66	1e-21
9	Right-Putamen	Right-Amygdala	M>F	7e-24	0.32	0.65	0.66	1e-20

10	rh.caudalmiddlefrontal	rh.posteriorcingulate	M<F	4e-23	0.31	0.66	0.66	7e-20
11	lh.posteriorcingulate	Left-Putamen	M<F	4e-23	0.31	0.65	0.66	9e-20
12	rh.parsopercularis	rh.inferiorparietal	M<F	5e-23	0.31	0.65	0.66	1e-19
13	rh.rostralanteriorcingulate	rh.caudalanteriorcingulate	M>F	1e-21	0.30	0.65	0.65	3e-18
14	lh.inferiorparietal	Left-Caudate	M<F	2e-21	0.30	0.65	0.65	4e-18
15	lh.caudalmiddlefrontal	lh.posteriorcingulate	M<F	2e-21	0.30	0.66	0.65	4e-18
16	lh.fusiform	Left-Hippocampus	M<F	3e-21	0.30	0.65	0.65	6e-18
17	rh.superiorparietal	Right-Caudate	M<F	4e-20	0.29	0.66	0.64	8e-17
18	lh.lateraloccipital	Left-Thalamus-Proper	M<F	7e-20	0.29	0.64	0.64	1e-16
19	lh.rostralanteriorcingulate	lh.caudalanteriorcingulate	M>F	8e-20	0.29	0.63	0.64	1e-16
20	rh.precentral	rh.posteriorcingulate	M<F	2e-19	0.28	0.64	0.64	4e-16
21	rh.fusiform	rh.bankssts	M<F	2e-19	0.28	0.64	0.64	4e-16
22	rh.superiortemporal	rh.transversetemporal	M>F	7e-19	0.28	0.64	0.64	1e-15
23	rh.precuneus	Right-Hippocampus	M<F	7e-19	0.28	0.65	0.64	1e-15
24	Left-Caudate	Left-Hippocampus	M<F	7e-19	0.28	0.65	0.64	1e-15
25	lh.parsopercularis	lh.supramarginal	M<F	1e-18	0.28	0.63	0.64	2e-15
26	lh.bankssts	Left-Hippocampus	M<F	1e-18	0.28	0.65	0.64	2e-15
27	Right-Caudate	lh.posteriorcingulate	M<F	1e-18	0.28	0.64	0.64	3e-15
28	lh.inferiortemporal	Left-Hippocampus	M<F	2e-18	0.28	0.64	0.64	3e-15
29	lh.superiorfrontal	lh.posteriorcingulate	M<F	3e-18	0.28	0.64	0.64	5e-15
30	Left-Putamen	Left-Amygdala	M>F	5e-18	0.27	0.64	0.64	1e-14
31	rh.parstriangularis	rh.supramarginal	M<F	8e-18	0.27	0.63	0.64	2e-14
32	lh.parsopercularis	lh.superiorparietal	M<F	1e-17	0.27	0.64	0.64	2e-14
33	rh.precuneus	rh.bankssts	M<F	1e-17	0.27	0.63	0.64	3e-14
34	rh.pericalcarine	rh.bankssts	M<F	2e-17	0.27	0.64	0.64	3e-14
35	rh.inferiortemporal	rh.bankssts	M<F	3e-17	0.27	0.64	0.63	6e-14
36	Right-Caudate	lh.rostralmiddlefrontal	M>F	3e-17	0.27	0.63	0.63	7e-14
37	lh.pericalcarine	Left-Thalamus-Proper	M<F	3e-17	0.27	0.63	0.63	7e-14
38	Right-Accumbens-area	Left-Thalamus-Proper	M>F	4e-17	0.27	0.64	0.63	7e-14
39	rh.insula	Right-Amygdala	M>F	5e-17	0.27	0.63	0.63	9e-14
40	lh.bankssts	Left-Caudate	M<F	5e-17	0.27	0.63	0.63	1e-13
41	lh.inferiorparietal	Left-Putamen	M<F	1e-16	0.26	0.64	0.63	3e-13
42	lh.lateraloccipital	lh.insula	M<F	2e-16	0.26	0.63	0.63	4e-13
43	lh.caudalmiddlefrontal	lh.caudalanteriorcingulate	M<F	2e-16	0.26	0.62	0.63	5e-13
44	rh.parsopercularis	rh.supramarginal	M<F	5e-16	0.26	0.64	0.63	1e-12
45	rh.rostralanteriorcingulate	Right-Caudate	M>F	6e-16	0.26	0.63	0.63	1e-12
46	rh.lateraloccipital	rh.bankssts	M<F	3e-15	0.25	0.63	0.63	7e-12
47	lh.isthmuscingulate	lh.bankssts	M<F	3e-15	0.25	0.63	0.63	7e-12
48	lh.bankssts	Left-Thalamus-Proper	M<F	3e-15	0.25	0.62	0.63	7e-12
49	Right-Caudate	Right-Hippocampus	M<F	3e-15	0.25	0.62	0.63	7e-12
50	rh.rostralmiddlefrontal	lh.caudalanteriorcingulate	M>F	3e-15	0.25	0.62	0.63	7e-12
51	rh.lingual	rh.bankssts	M<F	3e-15	0.26	0.64	0.63	7e-12
52	rh.precentral	rh.superiorparietal	M<F	4e-15	0.25	0.62	0.63	9e-12
53	Right-Caudate	lh.rostralanteriorcingulate	M>F	4e-15	0.25	0.64	0.62	9e-12
54	rh.precuneus	Right-Thalamus-Proper	M<F	4e-15	0.25	0.62	0.62	9e-12
55	rh.bankssts	Right-Caudate	M<F	8e-15	0.25	0.62	0.62	2e-11
56	lh.lingual	lh.insula	M<F	8e-15	0.25	0.63	0.62	2e-11
57	rh.inferiorparietal	Right-Caudate	M<F	8e-15	0.25	0.63	0.62	2e-11
58	lh.rostralmiddlefrontal	lh.superiorfrontal	M>F	8e-15	0.25	0.63	0.62	2e-11
59	rh.precentral	rh.postcentral	M<F	8e-15	0.25	0.63	0.62	2e-11
60	lh.superiorfrontal	lh.caudalmiddlefrontal	M<F	8e-15	0.25	0.62	0.62	2e-11
61	rh.isthmuscingulate	Right-Putamen	M<F	1e-14	0.25	0.62	0.62	2e-11
62	lh.pericalcarine	lh.insula	M<F	1e-14	0.25	0.61	0.62	2e-11
63	Left-Pallidum	Left-Amygdala	M>F	1e-14	0.25	0.63	0.62	2e-11
64	rh.parsopercularis	rh.precuneus	M<F	2e-14	0.25	0.62	0.62	3e-11
65	lh.precuneus	Left-Putamen	M<F	2e-14	0.24	0.62	0.62	4e-11

66	rh.parstriangularis	rh.postcentral	M<F	2e-14	0.24	0.62	0.62	4e-11
67	rh.fusiform	Right-Hippocampus	M<F	2e-14	0.24	0.63	0.62	5e-11
68	lh.parstriangularis	lh.supramarginal	M<F	2e-14	0.24	0.60	0.62	5e-11
69	lh.lingual	Left-Putamen	M<F	3e-14	0.24	0.61	0.62	6e-11
70	lh.postcentral	lh.superiortemporal	M<F	5e-14	0.24	0.61	0.62	9e-11
71	lh.lateraloccipital	Left-Caudate	M<F	7e-14	0.24	0.61	0.62	1e-10
72	rh.superiorfrontal	rh.rostralanteriorcingulate	M>F	7e-14	0.24	0.61	0.62	1e-10
73	rh.postcentral	rh.bankssts	M<F	9e-14	0.24	0.60	0.62	2e-10
74	lh.lingual	Left-Caudate	M<F	9e-14	0.24	0.62	0.62	2e-10
75	Right-Thalamus-Proper	Left-Putamen	M<F	1e-13	0.24	0.61	0.62	2e-10
76	rh.parsopercularis	rh.superiorparietal	M<F	1e-13	0.24	0.62	0.62	2e-10
77	lh.parsopercularis	lh.precuneus	M<F	1e-13	0.24	0.61	0.62	3e-10
78	lh.lateraloccipital	lh.transversetemporal	M<F	1e-13	0.24	0.61	0.62	3e-10
79	Right-Caudate	Left-Thalamus-Proper	M<F	1e-13	0.24	0.61	0.62	3e-10
80	rh.precentral	rh.inferiorparietal	M<F	1e-13	0.24	0.62	0.62	3e-10
81	lh.precuneus	Left-Thalamus-Proper	M<F	1e-13	0.24	0.63	0.62	3e-10
82	lh.precentral	lh.inferiorparietal	M<F	2e-13	0.24	0.63	0.62	3e-10
83	lh.lateraloccipital	Left-Putamen	M<F	2e-13	0.24	0.60	0.62	5e-10
84	rh.rostralanteriorcingulate	lh.caudalanteriorcingulate	M>F	3e-13	0.23	0.63	0.62	6e-10
85	lh.isthmuscingulate	Left-Caudate	M<F	3e-13	0.23	0.62	0.62	6e-10
86	rh.rostralmiddlefrontal	rh.inferiorparietal	M<F	3e-13	0.23	0.61	0.62	7e-10
87	lh.inferiortemporal	Left-Thalamus-Proper	M<F	5e-13	0.23	0.61	0.62	9e-10
88	lh.lingual	lh.superiortemporal	M<F	5e-13	0.23	0.61	0.62	1e-09
89	rh.rostralmiddlefrontal	Right-Caudate	M>F	6e-13	0.23	0.62	0.62	1e-09
90	lh.bankssts	lh.insula	M<F	6e-13	0.23	0.62	0.62	1e-09
91	rh.bankssts	Right-Hippocampus	M<F	7e-13	0.23	0.61	0.62	1e-09
92	lh.isthmuscingulate	Left-Putamen	M<F	8e-13	0.23	0.62	0.62	2e-09
93	lh.lingual	Left-Thalamus-Proper	M<F	8e-13	0.23	0.62	0.62	2e-09
94	Right-Thalamus-Proper	Right-Accumbens-area	M>F	8e-13	0.23	0.62	0.62	2e-09
95	rh.lingual	Right-Putamen	M<F	1e-12	0.23	0.61	0.61	2e-09
96	rh.lateraloccipital	rh.insula	M<F	1e-12	0.23	0.61	0.61	2e-09
97	lh.superiorfrontal	lh.rostralanteriorcingulate	M>F	1e-12	0.23	0.60	0.61	2e-09
98	rh.lateraloccipital	Right-Hippocampus	M<F	1e-12	0.23	0.62	0.61	2e-09
99	lh.caudalmiddlefrontal	lh.precentral	M<F	1e-12	0.23	0.62	0.61	2e-09
100	lh.rostralmiddlefrontal	lh.rostralanteriorcingulate	M>F	2e-12	0.23	0.61	0.61	3e-09
101	lh.precentral	lh.superiorparietal	M<F	2e-12	0.23	0.63	0.61	3e-09
102	lh.lingual	lh.bankssts	M<F	2e-12	0.23	0.62	0.61	3e-09
103	rh.middletemporal	rh.bankssts	M<F	2e-12	0.23	0.62	0.61	4e-09
104	lh.lingual	lh.transversetemporal	M<F	2e-12	0.23	0.61	0.61	4e-09
105	rh.posteriorcingulate	lh.caudalanteriorcingulate	M<F	2e-12	0.23	0.61	0.61	4e-09
106	rh.rostralmiddlefrontal	Left-Caudate	M>F	3e-12	0.23	0.61	0.61	6e-09
107	lh.caudalanteriorcingulate	Left-Putamen	M<F	3e-12	0.23	0.61	0.61	6e-09
108	rh.pericalcarine	Right-Hippocampus	M<F	3e-12	0.22	0.61	0.61	7e-09
109	rh.caudalanteriorcingulate	Right-Caudate	M>F	4e-12	0.22	0.61	0.61	7e-09
110	rh.parstriangularis	rh.superiorparietal	M<F	6e-12	0.22	0.59	0.61	1e-08
111	lh.superiorfrontal	lh.caudalanteriorcingulate	M<F	8e-12	0.22	0.61	0.61	2e-08
112	rh.lateraloccipital	Right-Putamen	M<F	8e-12	0.22	0.61	0.61	2e-08
113	lh.caudalanteriorcingulate	lh.superiorparietal	M<F	9e-12	0.22	0.59	0.61	2e-08
114	rh.isthmuscingulate	rh.bankssts	M<F	1e-11	0.22	0.61	0.61	2e-08
115	lh.rostralmiddlefrontal	Left-Caudate	M>F	1e-11	0.22	0.61	0.61	2e-08
116	rh.lingual	rh.insula	M<F	1e-11	0.22	0.62	0.61	2e-08
117	Left-Caudate	Left-Putamen	M<F	1e-11	0.22	0.61	0.61	3e-08
118	rh.rostralmiddlefrontal	rh.superiorfrontal	M>F	1e-11	0.22	0.60	0.61	3e-08
119	rh.isthmuscingulate	Right-Caudate	M<F	2e-11	0.22	0.61	0.61	4e-08
120	rh.superiorparietal	Right-Hippocampus	M<F	2e-11	0.22	0.62	0.61	4e-08
121	rh.middletemporal	Right-Caudate	M<F	2e-11	0.22	0.61	0.61	5e-08

122	lh.inferior temporal	lh.insula	M < F	4e-11	0.21	0.61	0.61	8e-08
123	lh.parstriangularis	lh.superior parietal	M < F	4e-11	0.21	0.58	0.61	9e-08
124	rh.pericalcarine	Right-Thalamus-Proper	M < F	6e-11	0.21	0.59	0.61	1e-07
125	rh.supramarginal	rh.lingual	M < F	7e-11	0.21	0.61	0.61	1e-07
126	rh.caudal anterior cingulate	lh.rostral anterior cingulate	M > F	7e-11	0.21	0.62	0.61	1e-07
127	rh.lateral occipital	Right-Thalamus-Proper	M < F	7e-11	0.21	0.60	0.61	1e-07
128	rh.lateral occipital	Right-Caudate	M < F	7e-11	0.21	0.60	0.61	1e-07
129	lh.insula	Left-Amygdala	M > F	7e-11	0.21	0.61	0.61	1e-07
130	lh.inferior temporal	lh.bankssts	M < F	7e-11	0.21	0.61	0.61	1e-07
131	rh.superior parietal	rh.bankssts	M < F	8e-11	0.21	0.61	0.61	2e-07
132	lh.isthmus cingulate	lh.superior parietal	M < F	9e-11	0.21	0.61	0.61	2e-07
133	rh.lateral occipital	rh.lingual	M < F	1e-10	0.21	0.62	0.61	2e-07
134	lh.rostral middle frontal	lh.supramarginal	M < F	1e-10	0.21	0.60	0.61	2e-07
135	rh.postcentral	rh.inferior parietal	M < F	1e-10	0.21	0.60	0.60	2e-07
136	lh.rostral middle frontal	lh.inferior parietal	M < F	1e-10	0.21	0.59	0.60	2e-07
137	lh.inferior temporal	Left-Caudate	M < F	1e-10	0.21	0.59	0.60	3e-07
138	rh.inferior parietal	Right-Thalamus-Proper	M < F	2e-10	0.21	0.59	0.60	3e-07
139	rh.posterior cingulate	lh.rostral middle frontal	M > F	2e-10	0.21	0.61	0.60	3e-07
140	rh.lingual	Right-Caudate	M < F	2e-10	0.21	0.61	0.60	3e-07
141	Right-Putamen	Left-Thalamus-Proper	M < F	2e-10	0.21	0.60	0.60	3e-07
142	lh.precentral	lh.posterior cingulate	M < F	2e-10	0.21	0.61	0.60	3e-07
143	lh.fusiform	lh.insula	M < F	2e-10	0.21	0.61	0.60	4e-07
144	lh.fusiform	lh.superior temporal	M < F	2e-10	0.21	0.61	0.60	4e-07
145	Right-Thalamus-Proper	lh.superior parietal	M < F	2e-10	0.21	0.60	0.60	5e-07
146	lh.precentral	lh.superior temporal	M < F	3e-10	0.21	0.58	0.60	5e-07
147	rh.pericalcarine	rh.insula	M < F	3e-10	0.21	0.59	0.60	5e-07
148	lh.precentral	lh.supramarginal	M < F	3e-10	0.21	0.60	0.60	5e-07
149	lh.lateral occipital	Left-Hippocampus	M < F	3e-10	0.21	0.61	0.60	6e-07
150	lh.middle temporal	Left-Hippocampus	M < F	3e-10	0.21	0.59	0.60	6e-07
151	rh.superior frontal	rh.precentral	M < F	3e-10	0.21	0.61	0.60	6e-07
152	Right-Thalamus-Proper	lh.precentral	M < F	3e-10	0.20	0.59	0.60	7e-07
153	lh.pericalcarine	lh.superior temporal	M < F	3e-10	0.20	0.61	0.60	7e-07
154	rh.isthmus cingulate	lh.isthmus cingulate	M < F	4e-10	0.20	0.59	0.60	7e-07
155	rh.fusiform	rh.middle temporal	M < F	4e-10	0.20	0.60	0.60	7e-07
156	lh.lateral occipital	lh.superior temporal	M < F	4e-10	0.20	0.61	0.60	7e-07
157	lh.superior temporal	lh.transverse temporal	M > F	4e-10	0.20	0.60	0.60	8e-07
158	Right-Pallidum	Right-Amygdala	M > F	4e-10	0.20	0.59	0.60	8e-07
159	rh.precentral	rh.bankssts	M < F	4e-10	0.20	0.58	0.60	9e-07
160	rh.parstriangularis	rh.inferior parietal	M < F	6e-10	0.20	0.58	0.60	1e-06
161	Left-Hippocampus	Left-Amygdala	M > F	7e-10	0.20	0.61	0.60	1e-06
162	lh.superior frontal	lh.precentral	M < F	8e-10	0.20	0.60	0.60	1e-06
163	rh.posterior cingulate	Left-Caudate	M < F	8e-10	0.20	0.60	0.60	1e-06
164	lh.bankssts	Left-Putamen	M < F	8e-10	0.20	0.60	0.60	2e-06
165	rh.rostral middle frontal	lh.posterior cingulate	M > F	8e-10	0.20	0.61	0.60	2e-06
166	lh.isthmus cingulate	lh.precuneus	M < F	9e-10	0.20	0.60	0.60	2e-06
167	rh.supramarginal	rh.precuneus	M < F	1e-09	0.20	0.61	0.60	2e-06
168	lh.superior parietal	Left-Thalamus-Proper	M < F	1e-09	0.20	0.58	0.60	2e-06
169	rh.superior frontal	rh.posterior cingulate	M < F	1e-09	0.20	0.60	0.60	2e-06
170	rh.precentral	Left-Thalamus-Proper	M < F	1e-09	0.20	0.59	0.60	2e-06
171	rh.precentral	rh.supramarginal	M < F	1e-09	0.20	0.59	0.60	3e-06
172	rh.precuneus	rh.insula	M < F	2e-09	0.20	0.60	0.60	3e-06
173	Left-Pallidum	Left-Hippocampus	M > F	2e-09	0.20	0.60	0.60	3e-06
174	lh.inferior temporal	lh.transverse temporal	M < F	2e-09	0.20	0.59	0.60	3e-06
175	rh.precentral	Left-Caudate	M < F	2e-09	0.20	0.59	0.60	3e-06
176	lh.precuneus	lh.bankssts	M < F	2e-09	0.20	0.60	0.60	3e-06
177	lh.fusiform	Left-Caudate	M < F	2e-09	0.20	0.59	0.60	3e-06

178	Left-Thalamus-Proper	Left-Hippocampus	M<F	2e-09	0.20	0.59	0.60	3e-06
179	lh.parstriangularis	lh.postcentral	M<F	3e-09	0.19	0.59	0.60	7e-06
180	lh.parstriangularis	lh.precentral	M<F	3e-09	0.19	0.59	0.60	7e-06
181	rh.middletemporal	Right-Hippocampus	M<F	4e-09	0.19	0.58	0.60	8e-06
182	lh.precuneus	Left-Hippocampus	M<F	4e-09	0.19	0.60	0.60	9e-06
183	rh.inferiortemporal	Right-Hippocampus	M<F	5e-09	0.19	0.60	0.60	9e-06
184	rh.insula	Right-Putamen	M>F	5e-09	0.19	0.60	0.60	1e-05
185	lh.cuneus	Left-Thalamus-Proper	M<F	5e-09	0.19	0.59	0.60	1e-05
186	lh.parstriangularis	lh.rostralmiddlefrontal	M>F	6e-09	0.19	0.60	0.60	1e-05
187	rh.parahippocampal	rh.bankssts	M<F	6e-09	0.19	0.59	0.60	1e-05
188	Right-Thalamus-Proper	lh.posteriorgcingulate	M<F	6e-09	0.19	0.59	0.60	1e-05
189	rh.superiorparietal	Left-Caudate	M<F	7e-09	0.19	0.57	0.60	1e-05
190	lh.superiorparietal	Left-Hippocampus	M<F	7e-09	0.19	0.61	0.60	1e-05
191	rh.cuneus	rh.bankssts	M<F	8e-09	0.19	0.60	0.60	1e-05
192	rh.lingual	rh.superiortemporal	M<F	8e-09	0.19	0.60	0.60	1e-05
193	Right-Hippocampus	Right-Amygdala	M>F	8e-09	0.19	0.60	0.59	2e-05

The fractional anisotropy (fa) weight function

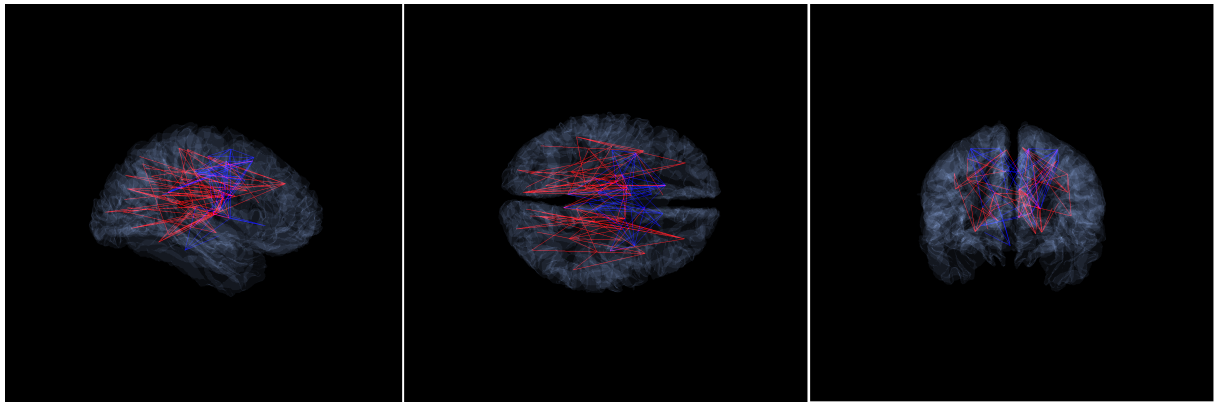


Figure S3. 120 sex impicator edges with the fractional anisotropy (fa) weight function with FWER $< 1.95 \times 10^{-5}$. Red color denotes edges where the higher fa weight implies the female sex, while blue edges correspond to those where higher fa weight implies the male sex (cf. Table S4). Three views correspond (from left to right) to sagittal, horizontal, and coronal positions. One may observe that red edges are mostly located in the posterior, while blue edges in the anterior lobes. Additionally, the inter-hemispheric edges are mostly blue ones. An animation of these images is available at <https://youtu.be/-bkB2qqXawY>.

Table S4: Sex impicator edges with the fractional anisotropy (fa) weight function

120 sex impicator edges with the fractional anisotropy (fa) weight function with FWER $< 1.95 \times 10^{-5}$. Index shows the ranking, *Vertex 1* and *Vertex 2* are the corresponding brain areas, $M>F$ indicates an edge with weight function significantly higher in males, while $M<F$ indicates an edge with weight function significantly higher in females. The $p_{.ks}$ and $D_{.ks}$ mean the Kolmogorov-Smirnov p-value and statistics for an edge. ACC denotes the accuracy of the best separation, $ACC_{.ks}$ denotes the $\frac{1}{2}(1 + D_{.ks})$ KS estimation for best separation accuracy. $FWER$ in the k th row shows the FWER upper bound for the first k edges.

	Vertex 1	Vertex 2	Male ?	Female	p_ks	D_ks	ACC	ACC_ks	FWER
1	rh.caudalanteriorcingulate	lh.rostralmiddlefrontal	M>F		5e-25	0.32	0.66	0.66	1e-21
2	lh.parsopercularis	lh.inferiorparietal	M<F		2e-24	0.32	0.66	0.66	4e-21
3	lh.parsopercularis	lh.caudalmiddlefrontal	M<F		5e-23	0.31	0.65	0.65	1e-19
4	rh.rostralmiddlefrontal	rh.caudalmiddlefrontal	M>F		6e-23	0.31	0.67	0.65	1e-19
5	rh.superiorfrontal	Right-Thalamus-Proper	M>F		1e-22	0.31	0.65	0.65	2e-19
6	rh.superiorfrontal	rh.caudalmiddlefrontal	M>F		5e-22	0.30	0.66	0.65	1e-18
7	rh.parstriangularis	rh.precentral	M<F		1e-21	0.30	0.65	0.65	2e-18
8	rh.rostralmiddlefrontal	rh.superiorfrontal	M>F		3e-21	0.30	0.65	0.65	5e-18
9	rh.rostralmiddlefrontal	rh.caudalanteriorcingulate	M>F		9e-21	0.29	0.65	0.65	2e-17
10	Right-Putamen	Right-Amygdala	M>F		2e-19	0.29	0.63	0.64	3e-16
11	lh.parstriangularis	lh.precentral	M<F		3e-19	0.28	0.63	0.64	7e-16
12	rh.parsopercularis	rh.precentral	M<F		4e-19	0.28	0.65	0.64	8e-16
13	rh.insula	Right-Amygdala	M>F		2e-18	0.28	0.63	0.64	4e-15
14	rh.rostralanteriorcingulate	rh.caudalanteriorcingulate	M>F		3e-18	0.28	0.63	0.64	5e-15
15	rh.rostralmiddlefrontal	lh.caudalanteriorcingulate	M>F		3e-18	0.28	0.64	0.64	5e-15
16	rh.rostralmiddlefrontal	rh.posteriorcingulate	M>F		4e-18	0.27	0.64	0.64	8e-15
17	rh.rostralmiddlefrontal	Right-Caudate	M>F		2e-17	0.27	0.63	0.63	4e-14
18	Right-Accumbens-area	Left-Thalamus-Proper	M>F		2e-17	0.27	0.64	0.63	4e-14
19	rh.parstriangularis	rh.postcentral	M<F		3e-17	0.27	0.63	0.63	6e-14
20	rh.superiorfrontal	rh.caudalanteriorcingulate	M>F		4e-17	0.27	0.63	0.63	8e-14
21	rh.lingual	rh.insula	M<F		1e-16	0.26	0.62	0.63	2e-13
22	lh.superiorfrontal	Left-Thalamus-Proper	M>F		3e-16	0.26	0.62	0.63	6e-13
23	rh.superiorfrontal	Right-Caudate	M>F		3e-15	0.25	0.62	0.63	7e-12
24	rh.rostralmiddlefrontal	Left-Caudate	M>F		3e-15	0.25	0.63	0.63	7e-12
25	Right-Thalamus-Proper	Right-Putamen	M<F		3e-15	0.26	0.63	0.63	7e-12
26	rh.rostralmiddlefrontal	Right-Thalamus-Proper	M>F		3e-15	0.26	0.64	0.63	7e-12
27	rh.parstriangularis	rh.supramarginal	M<F		4e-15	0.25	0.62	0.62	9e-12
28	lh.parsopercularis	lh.precentral	M<F		8e-15	0.25	0.62	0.62	2e-11
29	lh.lingual	Left-Caudate	M<F		1e-14	0.25	0.62	0.62	2e-11
30	rh.precuneus	Right-Putamen	M<F		1e-14	0.25	0.63	0.62	2e-11
31	rh.superiorfrontal	Right-Pallidum	M>F		1e-14	0.25	0.63	0.62	2e-11
32	Right-Caudate	lh.rostralanteriorcingulate	M>F		1e-14	0.25	0.63	0.62	2e-11
33	lh.superiorfrontal	Left-Pallidum	M>F		2e-14	0.25	0.62	0.62	3e-11
34	rh.rostralmiddlefrontal	lh.posteriorcingulate	M>F		3e-14	0.24	0.63	0.62	7e-11
35	rh.precentral	rh.postcentral	M<F		4e-14	0.24	0.63	0.62	7e-11
36	Left-Putamen	Left-Amygdala	M>F		6e-14	0.24	0.61	0.62	1e-10
37	lh.postcentral	lh.superiortemporal	M<F		6e-14	0.24	0.61	0.62	1e-10
38	Left-Pallidum	Left-Amygdala	M>F		8e-14	0.24	0.61	0.62	2e-10
39	lh.lingual	lh.insula	M<F		1e-13	0.24	0.61	0.62	2e-10
40	lh.parsopercularis	lh.insula	M<F		1e-13	0.24	0.62	0.62	3e-10
41	rh.superiorfrontal	rh.paracentral	M<F		2e-13	0.24	0.62	0.62	3e-10
42	Right-Putamen	Right-Pallidum	M<F		2e-13	0.24	0.62	0.62	4e-10
43	Right-Caudate	lh.rostralmiddlefrontal	M>F		2e-13	0.24	0.60	0.62	4e-10
44	rh.postcentral	rh.bankssts	M<F		3e-13	0.24	0.60	0.62	5e-10
45	lh.rostralmiddlefrontal	lh.superiorfrontal	M>F		3e-13	0.24	0.62	0.62	5e-10
46	rh.rostralanteriorcingulate	lh.caudalanteriorcingulate	M>F		3e-13	0.23	0.63	0.62	6e-10
47	lh.lingual	lh.transversetemporal	M<F		7e-13	0.23	0.61	0.62	1e-09
48	rh.pericalcarine	Right-Hippocampus	M<F		1e-12	0.23	0.62	0.61	2e-09
49	rh.lingual	Right-Caudate	M<F		1e-12	0.23	0.62	0.61	2e-09
50	lh.rostralanteriorcingulate	lh.caudalanteriorcingulate	M>F		2e-12	0.23	0.59	0.61	4e-09
51	rh.caudalmiddlefrontal	Right-Thalamus-Proper	M>F		2e-12	0.23	0.62	0.61	4e-09
52	rh.superiorfrontal	rh.rostralanteriorcingulate	M>F		2e-12	0.23	0.60	0.61	4e-09
53	rh.posteriorcingulate	Right-Hippocampus	M<F		3e-12	0.22	0.61	0.61	7e-09
54	Right-Thalamus-Proper	Right-Accumbens-area	M>F		4e-12	0.22	0.62	0.61	8e-09

55	rh.precuneus	rh.insula	M<F	5e-12	0.22	0.61	0.61	9e-09
56	Right-Thalamus-Proper	Right-Pallidum	M<F	5e-12	0.22	0.60	0.61	1e-08
57	rh.caudalmiddlefrontal	Right-Caudate	M>F	7e-12	0.22	0.61	0.61	1e-08
58	lh.parsopercularis	Left-Putamen	M<F	7e-12	0.22	0.61	0.61	1e-08
59	Left-Thalamus-Proper	Left-Putamen	M<F	8e-12	0.22	0.61	0.61	2e-08
60	rh.caudalmiddlefrontal	Right-Putamen	M>F	1e-11	0.22	0.62	0.61	2e-08
61	lh.rostralmiddlefrontal	lh.caudalmiddlefrontal	M>F	1e-11	0.22	0.61	0.61	3e-08
62	rh.superiorfrontal	Right-Putamen	M>F	1e-11	0.22	0.60	0.61	3e-08
63	Right-Thalamus-Proper	Left-Thalamus-Proper	M<F	2e-11	0.22	0.62	0.61	3e-08
64	lh.cuneus	Left-Thalamus-Proper	M<F	2e-11	0.22	0.61	0.61	4e-08
65	lh.lateraloccipital	Left-Caudate	M<F	2e-11	0.22	0.61	0.61	4e-08
66	rh.posteriorcingulate	Right-Thalamus-Proper	M<F	2e-11	0.22	0.60	0.61	4e-08
67	Right-Caudate	Left-Thalamus-Proper	M<F	2e-11	0.22	0.59	0.61	5e-08
68	lh.insula	Left-Amygdala	M>F	3e-11	0.22	0.61	0.61	5e-08
69	rh.superiorfrontal	rh.posteriorcingulate	M>F	4e-11	0.21	0.61	0.61	8e-08
70	Right-Hippocampus	lh.posteriorcingulate	M<F	4e-11	0.21	0.59	0.61	9e-08
71	rh.caudalanteriorcingulate	lh.rostralanteriorcingulate	M>F	5e-11	0.21	0.62	0.61	9e-08
72	lh.parstriangularis	lh.supramarginal	M<F	5e-11	0.21	0.59	0.61	1e-07
73	lh.superiorfrontal	lh.caudalmiddlefrontal	M>F	5e-11	0.21	0.61	0.61	1e-07
74	rh.posteriorcingulate	lh.rostralmiddlefrontal	M>F	6e-11	0.21	0.61	0.61	1e-07
75	lh.superiorfrontal	lh.rostralanteriorcingulate	M>F	7e-11	0.21	0.58	0.61	1e-07
76	rh.parstriangularis	rh.superiorparietal	M<F	8e-11	0.21	0.58	0.61	1e-07
77	rh.rostralanteriorcingulate	Right-Caudate	M>F	8e-11	0.21	0.59	0.61	2e-07
78	rh.isthmuscingulate	Right-Pallidum	M<F	8e-11	0.21	0.59	0.61	2e-07
79	lh.pericalcarine	Left-Thalamus-Proper	M<F	1e-10	0.21	0.61	0.61	2e-07
80	lh.caudalmiddlefrontal	lh.rostralanteriorcingulate	M<F	1e-10	0.21	0.59	0.61	2e-07
81	rh.parsopercularis	rh.postcentral	M<F	1e-10	0.21	0.62	0.61	2e-07
82	lh.rostralmiddlefrontal	lh.posteriorcingulate	M>F	1e-10	0.21	0.61	0.60	2e-07
83	lh.lingual	Left-Putamen	M<F	1e-10	0.21	0.61	0.60	2e-07
84	Right-Caudate	lh.precentral	M<F	1e-10	0.21	0.59	0.60	3e-07
85	lh.superiorfrontal	Left-Caudate	M>F	2e-10	0.21	0.60	0.60	3e-07
86	lh.lingual	lh.superiortemporal	M<F	2e-10	0.21	0.59	0.60	4e-07
87	rh.isthmuscingulate	Right-Thalamus-Proper	M<F	2e-10	0.21	0.60	0.60	4e-07
88	lh.parstriangularis	lh.postcentral	M<F	2e-10	0.21	0.59	0.60	4e-07
89	lh.pericalcarine	lh.insula	M<F	2e-10	0.21	0.60	0.60	4e-07
90	rh.posteriorcingulate	rh.isthmuscingulate	M<F	3e-10	0.21	0.59	0.60	5e-07
91	lh.precentral	lh.superiortemporal	M<F	3e-10	0.21	0.58	0.60	6e-07
92	rh.cuneus	rh.bankssts	M<F	4e-10	0.20	0.60	0.60	7e-07
93	Left-Hippocampus	Left-Amygdala	M>F	4e-10	0.20	0.60	0.60	7e-07
94	rh.lingual	Right-Putamen	M<F	4e-10	0.20	0.61	0.60	7e-07
95	lh.lateraloccipital	lh.transversetemporal	M<F	4e-10	0.20	0.60	0.60	7e-07
96	lh.caudalmiddlefrontal	Left-Thalamus-Proper	M>F	4e-10	0.20	0.61	0.60	8e-07
97	rh.parsopercularis	rh.precuneus	M<F	5e-10	0.20	0.61	0.60	1e-06
98	rh.precuneus	Right-Pallidum	M<F	6e-10	0.20	0.61	0.60	1e-06
99	rh.parstriangularis	rh.inferiorparietal	M<F	6e-10	0.20	0.58	0.60	1e-06
100	rh.caudalanteriorcingulate	lh.superiorfrontal	M>F	6e-10	0.20	0.59	0.60	1e-06
101	rh.precuneus	Right-Thalamus-Proper	M<F	7e-10	0.20	0.61	0.60	1e-06
102	rh.precentral	rh.bankssts	M<F	8e-10	0.20	0.58	0.60	2e-06
103	Right-Pallidum	Right-Amygdala	M>F	1e-09	0.20	0.59	0.60	2e-06
104	Right-Thalamus-Proper	lh.superiorparietal	M<F	1e-09	0.20	0.60	0.60	2e-06
105	lh.parstriangularis	lh.superiorparietal	M<F	1e-09	0.20	0.58	0.60	3e-06
106	lh.superiorfrontal	lh.caudalanteriorcingulate	M>F	2e-09	0.20	0.60	0.60	3e-06
107	rh.lingual	rh.superiortemporal	M<F	2e-09	0.20	0.59	0.60	3e-06
108	rh.insula	Right-Hippocampus	M<F	2e-09	0.20	0.59	0.60	5e-06
109	lh.parsopercularis	lh.precuneus	M<F	2e-09	0.20	0.60	0.60	5e-06
110	rh.rostralmiddlefrontal	rh.inferiorparietal	M<F	3e-09	0.20	0.59	0.60	5e-06

111	lh.lateraloccipital	Left-Putamen	M<F	3e-09	0.20	0.59	0.60	5e-06
112	Right-Thalamus-Proper	Right-Caudate	M<F	3e-09	0.19	0.60	0.60	6e-06
113	rh.supramarginal	rh.lingual	M<F	4e-09	0.19	0.59	0.60	7e-06
114	Right-Thalamus-Proper	lh.posteriorcingulate	M<F	5e-09	0.19	0.60	0.60	1e-05
115	rh.pericalcarine	rh.insula	M<F	5e-09	0.19	0.58	0.60	1e-05
116	rh.precuneus	Right-Caudate	M<F	9e-09	0.19	0.60	0.59	2e-05
117	rh.lingual	rh.transversetemporal	M<F	1e-08	0.19	0.58	0.59	2e-05
118	lh.fusiform	Left-Caudate	M<F	1e-08	0.19	0.59	0.59	2e-05
119	Right-Thalamus-Proper	Left-Putamen	M<F	1e-08	0.19	0.59	0.59	2e-05
120	lh.posteriorcingulate	Left-Thalamus-Proper	M<F	1e-08	0.19	0.60	0.59	2e-05

The fiber length (fl) weight function

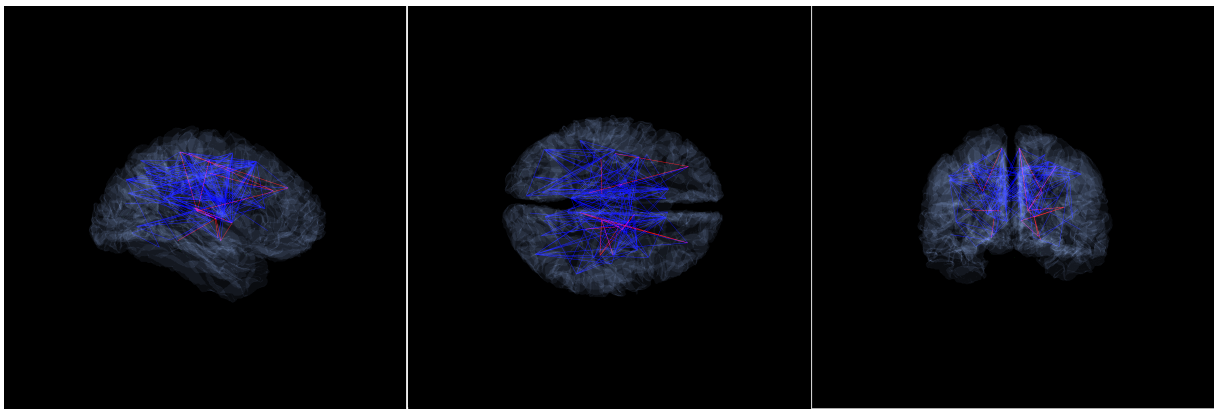


Figure S4. 207 sex impicator edges with the fiber length (fl) weight function with $\text{FWER} < 1.95 \times 10^{-5}$. Red color denotes edges where the higher fl weight implies the female sex, while blue edges correspond to those where higher fl weight implies the male sex (cf. Table S5). Three views correspond (from left to right) to sagittal, horizontal, and coronal positions. One may observe that most edges on the figure are blue, since – statistically – males have larger brain volumes than females. Most interestingly, there are several red edges on the figure, which are significantly longer in women than in men, and from their length, one can infer the sex of the subject with more than 60% correctness (e.g., between the Left-Putamen & Left-Hippocampus, or between right parsopercularis & right precentral areas). An animation of these images is available at <https://youtu.be/KVzP50pxU2E>.

Table S5: Sex impicator edges with the fiber length (fl) weight function

207 sex impicator edges with the fiber length (fl) weight function with $\text{FWER} < 1.95 \times 10^{-5}$. Index tells the ranking, *Vertex 1* and *Vertex 2* are the corresponding brain areas, $M>F$ indicates an edge with weight function significantly higher in males, while $M<F$ indicates an edge with weight function significantly higher in females. The *p_ks* and *D_ks* mean the Kolmogorov-Smirnov p-value and statistics for an edge. *ACC* denotes the accuracy of the best separation, *ACC_ks* denotes the $\frac{1}{2}(1+D_{\text{ks}})$ KS estimation for best separation accuracy. *FWER* in the *k*th row shows the FWER upper bound for the first *k* edges. In the statistical analysis only the edges were considered (i.e., where the fl weight function was positive).

	Vertex 1	Vertex 2	Male ? Female	p_ks	D_ks	ACC	ACC_ks	FWER
1	lh.superiorfrontal	lh.caudalanteriorcingulate	M>F	2e-42	0.42	0.71	0.71	3e-39
2	rh.superiorfrontal	rh.caudalanteriorcingulate	M>F	6e-38	0.40	0.70	0.70	1e-34
3	lh.caudalmiddlefrontal	lh.caudalanteriorcingulate	M>F	1e-31	0.36	0.68	0.68	2e-28
4	lh.superiorfrontal	Left-Pallidum	M>F	2e-30	0.37	0.69	0.68	3e-27

5	lh.caudalmiddlefrontal	lh.posteriorcingulate	M>F	7e-30	0.35	0.68	0.68	1e-26
6	rh.caudalmiddlefrontal	rh.posteriorcingulate	M>F	1e-29	0.35	0.69	0.68	2e-26
7	rh.superiorfrontal	Right-Pallidum	M>F	2e-27	0.35	0.68	0.68	4e-24
8	rh.rostralmiddlefrontal	rh.caudalanteriorcingulate	M>F	3e-26	0.33	0.67	0.67	6e-23
9	lh.superiorfrontal	lh.posteriorcingulate	M>F	5e-25	0.32	0.67	0.66	1e-21
10	rh.superiorfrontal	Right-Thalamus-Proper	M>F	3e-24	0.32	0.66	0.66	6e-21
11	lh.superiorfrontal	lh.caudalmiddlefrontal	M>F	4e-24	0.32	0.67	0.66	9e-21
12	rh.superiorfrontal	Right-Putamen	M>F	1e-23	0.31	0.66	0.66	2e-20
13	lh.posteriorcingulate	Left-Pallidum	M>F	6e-23	0.31	0.66	0.66	1e-19
14	lh.precentral	Left-Thalamus-Proper	M>F	1e-22	0.31	0.66	0.65	2e-19
15	rh.precentral	Right-Thalamus-Proper	M>F	1e-21	0.30	0.66	0.65	2e-18
16	lh.posteriorcingulate	Left-Putamen	M>F	2e-21	0.30	0.66	0.65	3e-18
17	rh.parsopercularis	Right-Putamen	M>F	4e-21	0.30	0.65	0.65	8e-18
18	lh.superiorfrontal	Left-Putamen	M>F	9e-21	0.29	0.65	0.65	2e-17
19	rh.posteriorcingulate	Right-Pallidum	M>F	3e-20	0.29	0.65	0.65	5e-17
20	rh.superiorfrontal	Right-Caudate	M>F	7e-20	0.29	0.66	0.64	1e-16
21	lh.isthmuscingulate	lh.superiorparietal	M>F	2e-19	0.29	0.64	0.64	3e-16
22	rh.parsopercularis	rh.precentral	M<F	2e-19	0.28	0.63	0.64	4e-16
23	lh.parstriangularis	Left-Putamen	M>F	2e-19	0.30	0.65	0.65	4e-16
24	lh.rostralmiddlefrontal	Left-Thalamus-Proper	M>F	3e-19	0.29	0.64	0.64	6e-16
25	lh.postcentral	Left-Thalamus-Proper	M>F	4e-19	0.28	0.63	0.64	8e-16
26	lh.caudalanteriorcingulate	Left-Caudate	M>F	5e-19	0.28	0.66	0.64	1e-15
27	lh.parsopercularis	lh.precentral	M<F	6e-19	0.28	0.62	0.64	1e-15
28	lh.superiorfrontal	Left-Caudate	M>F	2e-18	0.28	0.65	0.64	4e-15
29	lh.rostralmiddlefrontal	lh.caudalmiddlefrontal	M>F	3e-18	0.28	0.63	0.64	5e-15
30	rh.rostralmiddlefrontal	lh.caudalanteriorcingulate	M>F	6e-18	0.37	0.68	0.68	1e-14
31	rh.superiorfrontal	rh.caudalmiddlefrontal	M>F	1e-17	0.27	0.64	0.64	2e-14
32	rh.rostralmiddlefrontal	Right-Thalamus-Proper	M>F	2e-17	0.28	0.64	0.64	3e-14
33	Right-Thalamus-Proper	lh.supramarginal	M>F	5e-17	0.51	0.77	0.76	1e-13
34	rh.parsopercularis	Right-Pallidum	M>F	5e-17	0.28	0.63	0.64	1e-13
35	rh.lateraloccipital	rh.lingual	M>F	7e-17	0.27	0.64	0.63	1e-13
36	Right-Caudate	lh.superiorfrontal	M>F	1e-16	0.30	0.65	0.65	2e-13
37	lh.caudalanteriorcingulate	Left-Pallidum	M>F	2e-16	0.29	0.66	0.65	4e-13
38	lh.rostralmiddlefrontal	lh.caudalanteriorcingulate	M>F	2e-16	0.38	0.69	0.69	4e-13
39	rh.rostralmiddlefrontal	Right-Putamen	M>F	4e-16	0.32	0.66	0.66	9e-13
40	rh.superiorfrontal	rh.posteriorcingulate	M>F	4e-16	0.34	0.68	0.67	9e-13
41	rh.superiorparietal	Right-Hippocampus	M>F	4e-16	0.29	0.65	0.64	9e-13
42	lh.paracentral	Left-Thalamus-Proper	M>F	4e-16	0.25	0.63	0.63	9e-13
43	rh.rostralmiddlefrontal	rh.posteriorcingulate	M>F	4e-16	0.26	0.64	0.63	9e-13
44	rh.rostralmiddlefrontal	Right-Caudate	M>F	4e-16	0.29	0.65	0.65	9e-13
45	lh.rostralmiddlefrontal	Left-Caudate	M>F	4e-16	0.34	0.67	0.67	9e-13
46	lh.inferiorparietal	Left-Thalamus-Proper	M>F	4e-16	0.27	0.64	0.63	9e-13
47	rh.caudalmiddlefrontal	rh.caudalanteriorcingulate	M>F	4e-16	0.29	0.66	0.65	9e-13
48	rh.postcentral	Right-Thalamus-Proper	M>F	4e-16	0.28	0.64	0.64	9e-13
49	lh.superiorfrontal	Left-Thalamus-Proper	M>F	4e-16	0.26	0.64	0.63	9e-13
50	lh.rostralmiddlefrontal	Left-Putamen	M>F	4e-16	0.31	0.65	0.66	9e-13
51	rh.rostralmiddlefrontal	rh.supramarginal	M>F	7e-16	0.30	0.66	0.65	1e-12
52	Right-Thalamus-Proper	lh.superiorfrontal	M>F	7e-16	0.37	0.69	0.68	1e-12
53	lh.rostralmiddlefrontal	lh.superiorparietal	M>F	8e-16	0.32	0.67	0.66	2e-12
54	lh.caudalanteriorcingulate	lh.superiorparietal	M>F	9e-16	0.31	0.66	0.66	2e-12
55	rh.caudalanteriorcingulate	rh.postcentral	M>F	1e-15	0.33	0.67	0.66	2e-12
56	lh.rostralmiddlefrontal	Left-Pallidum	M>F	1e-15	0.28	0.64	0.64	3e-12
57	lh.caudalanteriorcingulate	lh.postcentral	M>F	1e-15	0.27	0.63	0.64	3e-12
58	rh.superiorparietal	rh.bankssts	M>F	1e-15	0.26	0.63	0.63	3e-12
59	rh.caudalmiddlefrontal	rh.paracentral	M>F	1e-15	0.26	0.64	0.63	3e-12
60	lh.superiortemporal	Left-Putamen	M<F	2e-15	0.26	0.63	0.63	3e-12

61	rh.rostralmiddlefrontal	Right-Pallidum	M>F	2e-15	0.30	0.65	0.65	4e-12
62	lh.rostralmiddlefrontal	lh.postcentral	M>F	3e-15	0.28	0.65	0.64	5e-12
63	rh.rostralmiddlefrontal	lh.caudalmiddlefrontal	M>F	3e-15	0.66	0.82	0.83	6e-12
64	rh.posteriorcingulate	lh.rostralmiddlefrontal	M>F	3e-15	0.39	0.70	0.70	6e-12
65	lh.superiorparietal	Left-Thalamus-Proper	M>F	3e-15	0.25	0.63	0.63	7e-12
66	lh.parsopercularis	lh.insula	M<F	3e-15	0.25	0.62	0.63	7e-12
67	rh.precentral	Right-Pallidum	M>F	5e-15	0.25	0.63	0.63	9e-12
68	rh.superiorfrontal	lh.caudalanteriorcingulate	M>F	5e-15	0.33	0.67	0.67	1e-11
69	lh.inferiorparietal	lh.transversetemporal	M>F	6e-15	0.25	0.62	0.63	1e-11
70	Right-Hippocampus	Left-Thalamus-Proper	M>F	7e-15	0.26	0.63	0.63	1e-11
71	lh.lateraloccipital	lh.lingual	M>F	8e-15	0.25	0.63	0.62	2e-11
72	lh.superiorparietal	Left-Hippocampus	M>F	8e-15	0.25	0.64	0.62	2e-11
73	rh.precentral	Left-Thalamus-Proper	M>F	9e-15	0.40	0.71	0.70	2e-11
74	Right-Thalamus-Proper	lh.superiorparietal	M>F	9e-15	0.36	0.71	0.68	2e-11
75	rh.superiorfrontal	lh.posteriorcingulate	M>F	2e-14	0.35	0.68	0.68	3e-11
76	rh.isthmuscingulate	rh.bankssts	M>F	2e-14	0.25	0.63	0.63	4e-11
77	rh.precentral	rh.posteriorcingulate	M>F	2e-14	0.24	0.63	0.62	4e-11
78	rh.caudalanteriorcingulate	lh.superiorfrontal	M>F	3e-14	0.29	0.66	0.65	6e-11
79	rh.precuneus	rh.bankssts	M>F	3e-14	0.24	0.63	0.62	7e-11
80	rh.fusiform	rh.inferiortemporal	M>F	4e-14	0.24	0.63	0.62	8e-11
81	rh.rostralmiddlefrontal	Left-Caudate	M>F	5e-14	0.32	0.68	0.66	1e-10
82	rh.posteriorcingulate	Right-Putamen	M>F	6e-14	0.24	0.62	0.62	1e-10
83	rh.paracentral	rh.caudalanteriorcingulate	M>F	6e-14	0.28	0.65	0.64	1e-10
84	rh.isthmuscingulate	rh.superiorparietal	M>F	7e-14	0.24	0.62	0.62	1e-10
85	Right-Putamen	Right-Hippocampus	M<F	7e-14	0.24	0.63	0.62	1e-10
86	rh.rostralmiddlefrontal	rh.superiorparietal	M>F	8e-14	0.27	0.65	0.63	2e-10
87	rh.lateraloccipital	rh.bankssts	M>F	1e-13	0.24	0.64	0.62	2e-10
88	Right-Thalamus-Proper	Left-Hippocampus	M>F	1e-13	0.26	0.64	0.63	2e-10
89	rh.caudalanteriorcingulate	lh.rostralmiddlefrontal	M>F	1e-13	0.32	0.67	0.66	2e-10
90	rh.posteriorcingulate	Right-Caudate	M>F	1e-13	0.24	0.64	0.62	3e-10
91	lh.posteriorcingulate	Left-Thalamus-Proper	M>F	2e-13	0.24	0.61	0.62	3e-10
92	lh.isthmuscingulate	lh.inferiorparietal	M>F	2e-13	0.24	0.62	0.62	4e-10
93	Left-Putamen	Left-Hippocampus	M<F	2e-13	0.24	0.62	0.62	4e-10
94	rh.precentral	rh.caudalanteriorcingulate	M>F	2e-13	0.24	0.62	0.62	4e-10
95	rh.posteriorcingulate	lh.superiorfrontal	M>F	3e-13	0.31	0.66	0.66	5e-10
96	rh.caudalanteriorcingulate	Right-Pallidum	M>F	3e-13	0.27	0.64	0.64	5e-10
97	rh.precuneus	rh.transversetemporal	M>F	3e-13	0.24	0.63	0.62	6e-10
98	rh.superiorfrontal	Left-Caudate	M>F	4e-13	0.31	0.66	0.65	7e-10
99	rh.parstriangularis	rh.rostralmiddlefrontal	M>F	4e-13	0.24	0.61	0.62	8e-10
100	lh.superiortemporal	Left-Pallidum	M<F	4e-13	0.26	0.63	0.63	8e-10
101	rh.fusiform	rh.bankssts	M>F	5e-13	0.24	0.62	0.62	9e-10
102	lh.rostralmiddlefrontal	lh.supramarginal	M>F	7e-13	0.26	0.65	0.63	1e-09
103	rh.caudalanteriorcingulate	rh.superiorparietal	M>F	7e-13	0.26	0.63	0.63	1e-09
104	rh.caudalanteriorcingulate	Right-Caudate	M>F	8e-13	0.23	0.63	0.62	1e-09
105	lh.caudalmiddlefrontal	lh.paracentral	M>F	9e-13	0.23	0.62	0.62	2e-09
106	rh.posteriorcingulate	Left-Caudate	M>F	1e-12	0.24	0.63	0.62	2e-09
107	lh.caudalmiddlefrontal	lh.insula	M<F	1e-12	0.23	0.60	0.61	2e-09
108	lh.caudalanteriorcingulate	Left-Thalamus-Proper	M>F	1e-12	0.23	0.63	0.62	2e-09
109	lh.caudalmiddlefrontal	Left-Caudate	M>F	1e-12	0.23	0.62	0.61	2e-09
110	rh.parstriangularis	Right-Putamen	M>F	2e-12	0.24	0.63	0.62	3e-09
111	rh.supramarginal	Right-Thalamus-Proper	M>F	2e-12	0.23	0.61	0.61	4e-09
112	lh.rostralmiddlefrontal	lh.precentral	M>F	2e-12	0.23	0.63	0.61	4e-09
113	lh.fusiform	lh.middletemporal	M>F	2e-12	0.23	0.61	0.61	5e-09
114	lh.precentral	lh.caudalanteriorcingulate	M>F	2e-12	0.23	0.63	0.61	5e-09
115	rh.superiorfrontal	Left-Thalamus-Proper	M>F	3e-12	0.40	0.68	0.70	5e-09
116	rh.inferiorparietal	Right-Thalamus-Proper	M>F	3e-12	0.23	0.62	0.61	6e-09

117	rh.postcentral	Right-Pallidum	M>F	4e-12	0.23	0.62	0.61	8e-09
118	lh.parstriangularis	Left-Caudate	M>F	4e-12	0.23	0.62	0.62	8e-09
119	Left-Pallidum	Left-Hippocampus	M<F	5e-12	0.24	0.61	0.62	9e-09
120	lh.isthmuscingulate	lh.bankssts	M>F	5e-12	0.23	0.64	0.61	9e-09
121	lh.precentral	lh.insula	M<F	5e-12	0.22	0.60	0.61	9e-09
122	lh.rostralmiddlefrontal	lh.paracentral	M>F	5e-12	0.27	0.64	0.63	1e-08
123	lh.paracentral	lh.caudalanteriorcingulate	M>F	5e-12	0.24	0.64	0.62	1e-08
124	rh.superiorfrontal	rh.postcentral	M>F	6e-12	0.22	0.62	0.61	1e-08
125	rh.rostralmiddlefrontal	rh.postcentral	M>F	8e-12	0.23	0.62	0.61	2e-08
126	rh.caudalanteriorcingulate	Left-Caudate	M>F	8e-12	0.22	0.61	0.61	2e-08
127	lh.insula	Left-Putamen	M<F	8e-12	0.22	0.62	0.61	2e-08
128	rh.isthmuscingulate	rh.inferiorparietal	M>F	9e-12	0.22	0.61	0.61	2e-08
129	rh.caudalanteriorcingulate	rh.supramarginal	M>F	9e-12	0.25	0.63	0.63	2e-08
130	rh.precentral	Left-Caudate	M>F	1e-11	0.34	0.69	0.67	2e-08
131	lh.parstriangularis	lh.rostralmiddlefrontal	M>F	1e-11	0.22	0.61	0.61	2e-08
132	rh.superiorfrontal	rh.paracentral	M>F	1e-11	0.22	0.62	0.61	3e-08
133	Right-Caudate	lh.rostralmiddlefrontal	M>F	1e-11	0.26	0.64	0.63	3e-08
134	lh.parsopercularis	lh.rostralmiddlefrontal	M>F	2e-11	0.22	0.60	0.61	3e-08
135	rh.posteriorcingulate	lh.caudalanteriorcingulate	M>F	2e-11	0.23	0.61	0.61	4e-08
136	lh.precentral	lh.inferiorparietal	M>F	2e-11	0.23	0.64	0.62	4e-08
137	lh.supramarginal	Left-Thalamus-Proper	M>F	2e-11	0.22	0.61	0.61	4e-08
138	lh.caudalanteriorcingulate	Left-Putamen	M>F	2e-11	0.22	0.62	0.61	5e-08
139	lh.parsopercularis	rh.caudalmiddlefrontal	M<F	3e-11	0.22	0.60	0.61	7e-08
140	rh.postcentral	Right-Caudate	M>F	3e-11	0.22	0.62	0.61	7e-08
141	lh.caudalmiddlefrontal	Left-Pallidum	M>F	3e-11	0.22	0.60	0.61	7e-08
142	Right-Thalamus-Proper	lh.isthmuscingulate	M>F	4e-11	0.22	0.60	0.61	7e-08
143	rh.caudalmiddlefrontal	Right-Caudate	M>F	5e-11	0.21	0.61	0.61	9e-08
144	lh.lateraloccipital	Left-Thalamus-Proper	M>F	5e-11	0.22	0.62	0.61	1e-07
145	Right-Caudate	lh.caudalanteriorcingulate	M>F	5e-11	0.21	0.61	0.61	1e-07
146	Right-Hippocampus	lh.posteriorcingulate	M>F	5e-11	0.24	0.63	0.62	1e-07
147	lh.parstriangularis	Left-Thalamus-Proper	M>F	5e-11	0.32	0.66	0.66	1e-07
148	lh.rostralmiddlefrontal	lh.posteriorcingulate	M>F	6e-11	0.21	0.60	0.61	1e-07
149	Right-Thalamus-Proper	Left-Thalamus-Proper	M>F	6e-11	0.21	0.61	0.61	1e-07
150	Right-Thalamus-Proper	lh.inferiorparietal	M>F	6e-11	0.38	0.71	0.69	1e-07
151	rh.posteriorcingulate	lh.isthmuscingulate	M>F	8e-11	0.22	0.61	0.61	1e-07
152	lh.bankssts	Left-Hippocampus	M>F	9e-11	0.21	0.60	0.61	2e-07
153	lh.caudalmiddlefrontal	lh.precentral	M>F	9e-11	0.21	0.60	0.61	2e-07
154	Left-Caudate	Left-Pallidum	M>F	1e-10	0.21	0.60	0.61	2e-07
155	rh.lateraloccipital	rh.transversetemporal	M>F	1e-10	0.26	0.65	0.63	2e-07
156	rh.lateraloccipital	Right-Thalamus-Proper	M>F	1e-10	0.23	0.63	0.61	2e-07
157	rh.superiorfrontal	rh.precentral	M>F	1e-10	0.21	0.61	0.60	2e-07
158	Right-Thalamus-Proper	lh.precentral	M>F	1e-10	0.32	0.68	0.66	2e-07
159	rh.rostralmiddlefrontal	rh.inferiorparietal	M>F	1e-10	0.31	0.70	0.66	2e-07
160	rh.parsopercularis	rh.caudalanteriorcingulate	M>F	1e-10	0.21	0.60	0.61	2e-07
161	rh.caudalmiddlefrontal	Left-Caudate	M>F	1e-10	0.24	0.61	0.62	3e-07
162	rh.paracentral	Right-Putamen	M>F	1e-10	0.21	0.60	0.60	3e-07
163	rh.inferiorparietal	Left-Thalamus-Proper	M>F	2e-10	0.40	0.71	0.70	3e-07
164	rh.caudalanteriorcingulate	lh.caudalanteriorcingulate	M>F	2e-10	0.21	0.60	0.61	3e-07
165	lh.precentral	Left-Pallidum	M>F	3e-10	0.21	0.61	0.60	6e-07
166	rh.superiortemporal	rh.insula	M<F	4e-10	0.21	0.59	0.60	7e-07
167	Right-Caudate	lh.precentral	M>F	5e-10	0.27	0.66	0.64	9e-07
168	rh.precuneus	rh.superiortemporal	M>F	5e-10	0.20	0.62	0.60	9e-07
169	rh.lingual	rh.bankssts	M>F	6e-10	0.20	0.60	0.60	1e-06
170	rh.superiorparietal	Left-Thalamus-Proper	M>F	6e-10	0.34	0.68	0.67	1e-06
171	Right-Caudate	lh.caudalmiddlefrontal	M>F	6e-10	0.21	0.61	0.61	1e-06
172	rh.isthmuscingulate	Left-Thalamus-Proper	M>F	6e-10	0.21	0.60	0.61	1e-06

173	Right-Thalamus-Proper	Right-Hippocampus	M>F	7e-10	0.20	0.60	0.60	1e-06
174	rh.lateraloccipital	rh.insula	M>F	8e-10	0.22	0.62	0.61	2e-06
175	rh.precuneus	Right-Thalamus-Proper	M>F	8e-10	0.20	0.61	0.60	2e-06
176	lh.postcentral	lh.inferiorparietal	M>F	9e-10	0.20	0.60	0.60	2e-06
177	rh.superiorparietal	Right-Thalamus-Proper	M>F	1e-09	0.20	0.61	0.60	2e-06
178	rh.superiorparietal	rh.precuneus	M>F	1e-09	0.20	0.61	0.60	2e-06
179	lh.superiorparietal	lh.bankssts	M>F	1e-09	0.20	0.61	0.60	2e-06
180	lh.superiorparietal	lh.lingual	M>F	1e-09	0.20	0.60	0.60	3e-06
181	Right-Thalamus-Proper	Right-Amygdala	M>F	1e-09	0.23	0.61	0.62	3e-06
182	lh.caudalanteriorcingulate	lh.supramarginal	M>F	1e-09	0.24	0.63	0.62	3e-06
183	rh.caudalmiddlefrontal	rh.precentral	M>F	1e-09	0.20	0.60	0.60	3e-06
184	Right-Putamen	Right-Pallidum	M>F	2e-09	0.20	0.60	0.60	3e-06
185	lh.posteriorcingulate	lh.inferiorparietal	M>F	2e-09	0.20	0.62	0.60	4e-06
186	rh.precentral	rh.inferiorparietal	M>F	2e-09	0.20	0.62	0.60	4e-06
187	lh.parstriangularis	lh.superiorparietal	M>F	2e-09	0.45	0.81	0.73	4e-06
188	rh.posteriorcingulate	Right-Thalamus-Proper	M>F	2e-09	0.20	0.60	0.60	4e-06
189	rh.rostralmiddlefrontal	rh.precentral	M>F	3e-09	0.20	0.62	0.60	5e-06
190	lh.fusiform	Left-Putamen	M<F	3e-09	0.28	0.67	0.64	5e-06
191	rh.parstriangularis	Right-Thalamus-Proper	M>F	3e-09	0.29	0.65	0.64	5e-06
192	rh.rostralmiddlefrontal	rh.precuneus	M>F	3e-09	0.31	0.72	0.66	6e-06
193	rh.lateraloccipital	rh.superiortemporal	M>F	3e-09	0.22	0.63	0.61	6e-06
194	lh.parsopercularis	Left-Putamen	M>F	3e-09	0.19	0.59	0.60	6e-06
195	lh.superiorfrontal	lh.postcentral	M>F	3e-09	0.20	0.61	0.60	7e-06
196	rh.superiorparietal	rh.superiortemporal	M>F	4e-09	0.20	0.60	0.60	7e-06
197	lh.caudalmiddlefrontal	lh.postcentral	M>F	4e-09	0.19	0.60	0.60	7e-06
198	lh.inferiortemporal	Left-Thalamus-Proper	M>F	4e-09	0.20	0.60	0.60	8e-06
199	Right-Caudate	Right-Pallidum	M>F	4e-09	0.19	0.60	0.60	8e-06
200	Right-Caudate	lh.isthmuscingulate	M>F	5e-09	0.25	0.65	0.62	9e-06
201	lh.superiortemporal	lh.insula	M<F	6e-09	0.19	0.60	0.60	1e-05
202	lh.caudalmiddlefrontal	Left-Thalamus-Proper	M>F	6e-09	0.19	0.59	0.60	1e-05
203	lh.parsopercularis	lh.superiorparietal	M>F	6e-09	0.20	0.61	0.60	1e-05
204	lh.precuneus	Left-Thalamus-Proper	M>F	7e-09	0.19	0.61	0.60	1e-05
205	rh.precentral	rh.superiorparietal	M>F	8e-09	0.19	0.60	0.60	1e-05
206	rh.posteriorcingulate	Left-Thalamus-Proper	M>F	8e-09	0.19	0.59	0.60	2e-05
207	lh.precentral	lh.posteriorcingulate	M>F	9e-09	0.19	0.61	0.59	2e-05